WEAK DECAYS OF B_s MESONS

Vladimir Galkin

Computing Centre, RAS, Moscow

(in collaboration with Rudolf Faustov)

Faustov, Galkin — Phys. Rev. D, **87**, 034033 (2013)
Faustov, Galkin — Phys. Rev. D, **87**, 094028 (2013)

The Helmholtz International Summer School
"Physics of Heavy Quarks and Hadrons"
Dubna, July 15-28

PLAN

1. INTRODUCTION
2. RELATIVISTIC QUARK MODEL
   - Quasipotential equation and $q\bar{q}$ interaction potential
   - Matrix elements of the electroweak current between meson states
3. WEAK B_s DECAYS
   - Heavy-to-heavy semileptonic $B_s \to D_s$ decays
     - Decays to ground state D_s mesons
     - Decays to radially excited D_s mesons
     - Decays to orbitally excited D_s mesons
   - Heavy-to-light semileptonic $B_s \to K$ decays
     - Decays to ground state K mesons
     - Decays to orbitally excited K mesons
   - Rare B_s decays
     - Rare semileptonic $B_s \to \varphi(\eta)$ decays
     - Rare radiative B_s decays
4. CONCLUSIONS

INTRODUCTION

Why is it interesting and important to study weak B_s decays?

- Weak B_s decays are considerably less studied both experimentally and theoretically than weak B decays
- Significant experimental progress in last few years
  - Data from Tevatron
  - Belle data collected at $\Upsilon(10860)$ resonance
  - Precise and comprehensive data are expected from LHCb (several decays are already observed for the first time)
- Additional source for determination of the Cabibbo-Kobayashi-Maskawa (CKM) matrix elements
- Some decay modes are preferable for studying CP violation
- Test of the standard model and "new physics models"

Exclusive semileptonic B decays were previously considered in our model —
Ebert, Faustov, Galkin, Phys. Rev. D **75**, 074008 (2007)

In last two years new more precise data were published by Belle and BaBar for $B \to \pi(\rho) l \nu_l$ decays

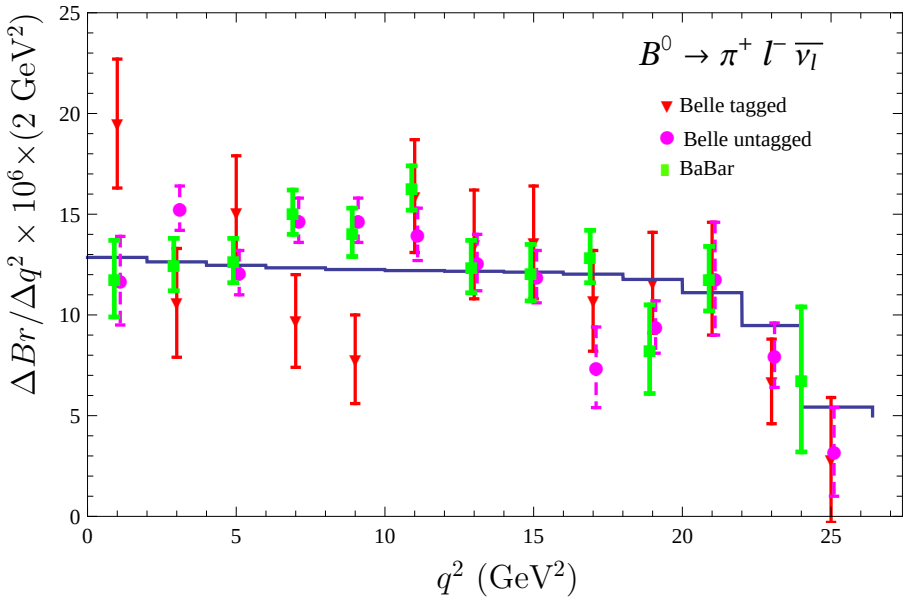

Figure 1: Comparison of predictions of our model with the recent experimental data (Belle 2011, 2013; BaBar 2012) for the $B^0 \longrightarrow \pi^+ l^- \nu$ decay.

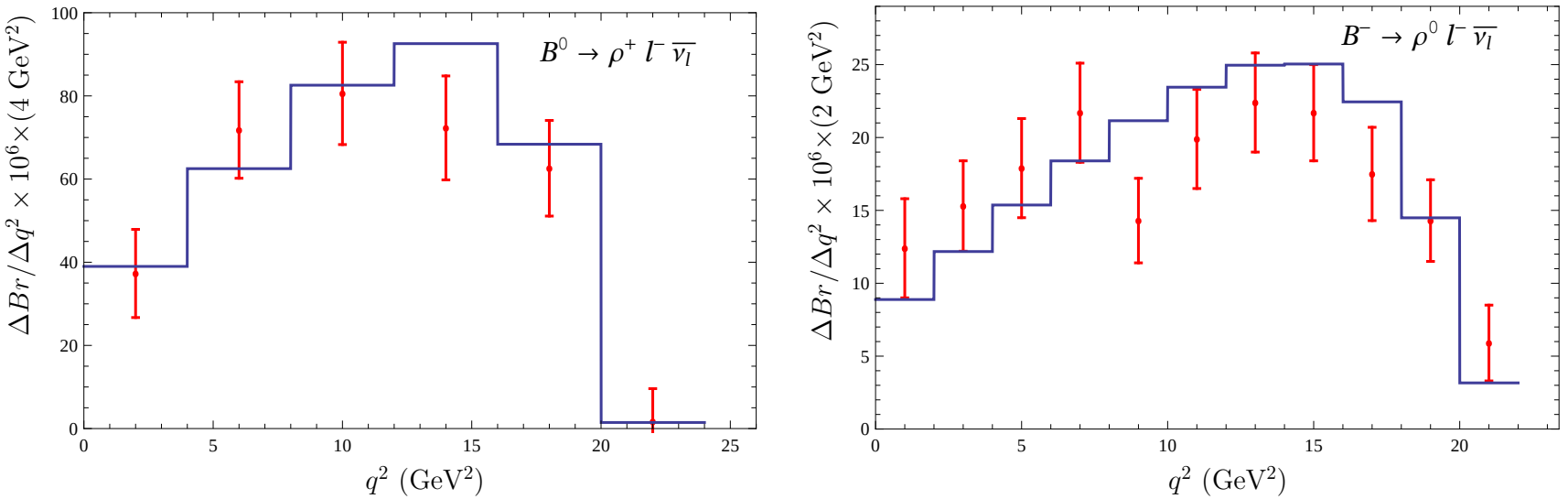

Figure 2: Comparison of predictions of our model with the recent Belle (2013) data for the $B \longrightarrow \rho l \nu$ decay.

The fit to the combined Belle and BaBar data yields

- from $B \to \pi l \nu_l$ decays

$$|V_{ub}| = (4.07 \pm 0.07_{\rm exp} \pm 0.21_{\rm theor}) \times 10^{-3}$$

- from $B \to \rho l \nu_l$ decays

$$|V_{ub}| = (4.03 \pm 0.15_{\rm exp} \pm 0.21_{\rm theor}) \times 10^{-3}$$

- from $B \to \pi l \nu_l$ and $B \to \rho l \nu_l$ decays

$$|V_{ub}| = (4.06 \pm 0.06_{\rm exp} \pm 0.21_{\rm theor}) \times 10^{-3}$$

Good agreement with the averaged value extracted from inclusive B decays

$$|V_{ub}| = (4.41 \pm 0.15^{+0.15}_{-0.19}) \times 10^{-3} \qquad (\rm PDG)$$

RELATIVISTIC QUARK MODEL

- **Quasipotential equation and $q\bar{q}$ interaction potential**

Quasipotential equation of Schrödinger type:

$$\left(\frac{b^2(M)}{2\mu_R} - \frac{\mathbf{p}^2}{2\mu_R}\right)\Psi_M(\mathbf{p}) = \int \frac{d^3q}{(2\pi)^3} V(\mathbf{p},\mathbf{q};M)\Psi_M(\mathbf{q})$$

$\mathbf{p}$ - relative momentum of quarks
M - bound state mass ($M = E_1 + E_2$)
μ_R - relativistic reduced mass:

$$\mu_R = \frac{E_1 E_2}{E_1 + E_2} = \frac{M^4 - (m_1^2 - m_2^2)^2}{4M^3}$$

$b(M)$ - on-mass-shell relative momentum in cms:

$$b^2(M) = \frac{[M^2 - (m_1 + m_2)^2][M^2 - (m_1 - m_2)^2]}{4M^2}$$

$E_{1,2}$ - center-of-mass energies:

$$E_1 = \frac{M^2 - m_2^2 + m_1^2}{2M}, \quad E_2 = \frac{M^2 - m_1^2 + m_2^2}{2M}$$

- $q\bar{q}$ **quasipotential**

(Constructed with the help of off-mass-shell scattering amplitude projected onto positive-energy states)

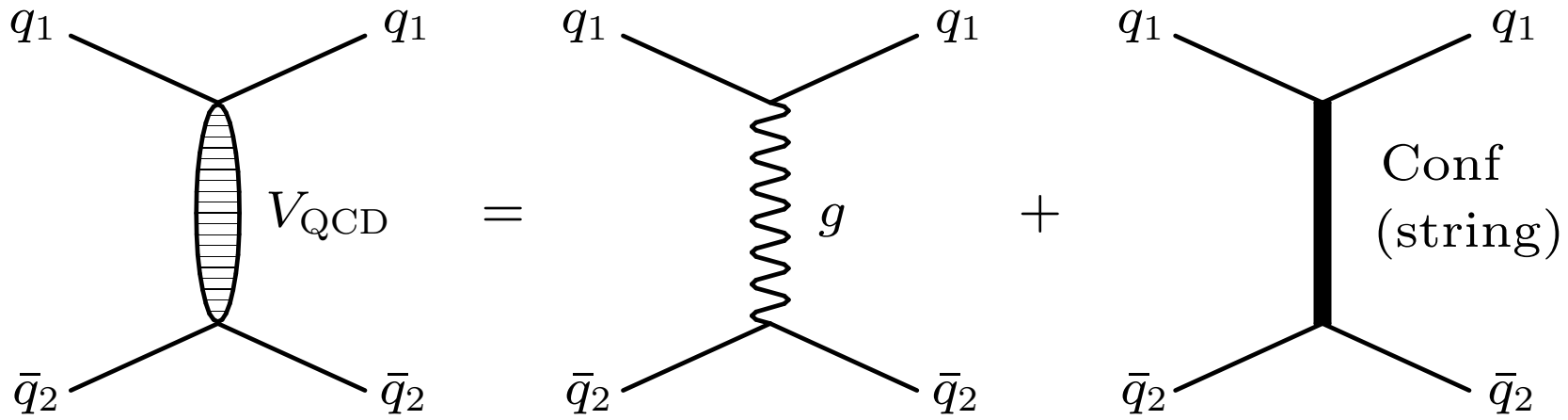

$$V(\mathbf{p},\mathbf{q};M) = \bar{u}_1(p)\bar{u}_2(-p)\left\{\frac{4}{3}\alpha_s D_{\mu\nu}(\mathbf{k})\gamma_1^\mu\gamma_2^\nu + V_{\rm conf}^V(\mathbf{k})\Gamma_1^\mu\Gamma_{2;\mu} + V_{\rm conf}^S(\mathbf{k})\right\}u_1(q)u_2(-q)$$

$\mathbf{k} = \mathbf{p} - \mathbf{q}$

$D_{\mu\nu}(\mathbf{k})$ - (perturbative) gluon propagator

$\Gamma_\mu(\mathbf{k})$ - effective long-range vertex with Pauli term:

$$\Gamma_\mu(\mathbf{k}) = \gamma_\mu + \frac{i\kappa}{2m}\sigma_{\mu\nu}k^\nu,$$

κ - anomalous chromomagnetic moment of quark,

$$u^{\lambda}(p) = \sqrt{\frac{\epsilon(p)+m}{2\epsilon(p)}} \begin{pmatrix} 1 \\ \dfrac{\boldsymbol{\sigma}\mathbf{p}}{\epsilon(p)+m} \end{pmatrix} \chi^{\lambda},$$

with $\epsilon(p) = \sqrt{\mathbf{p}^2 + m^2}$.

- Lorentz structure of $V_{\rm conf} = V^V_{\rm conf} + V^S_{\rm conf}$

In nonrelativistic limit

$$\left.\begin{array}{rcl} V^V_{\rm conf}(r) & = & (1-\varepsilon)(Ar+B) \\ V^S_{\rm conf}(r) & = & \varepsilon(Ar+B) \end{array}\right\} \quad \text{Sum}: \quad (Ar+B)$$

ε - mixing parameter

$$V_{\rm NR}(r) = V_{\rm Coul}(r) + V_{\rm conf}(r)$$

$$V_{\rm Coul}(r) = -\frac{4}{3}\frac{\alpha_s}{r}$$

Parameters A, B, κ, ε and quark masses fixed from analysis of meson masses and radiative decays:

$\varepsilon = -1$ from heavy quarkonium radiative decays ($J/\psi \to \eta_c + \gamma$) and HQET

$\kappa = -1$ from fine splitting of heavy quarkonium ^3P_J states and HQET

$(1+\kappa) = 0 \Longrightarrow$ vanishing long-range chromomagnetic interaction ! (flux tube model)

$$\alpha_s(\mu) = \frac{4\pi}{\beta_0 \ln \frac{\mu^2}{\Lambda^2}}, \quad \beta_0 = 11 - \frac{2}{3} n_f, \quad \mu = \frac{2 m_1 m_2}{m_1 + m_2},$$

Quasipotential parameters:

$A = 0.18$ GeV^2, $\quad B = -0.30$ GeV,

$\Lambda = 0.169$ GeV

Quark masses:

$m_b = 4.88$ GeV $\qquad m_s = 0.50$ GeV

$m_c = 1.55$ GeV $\qquad m_{u,d} = 0.33$ GeV

• Matrix elements of the electroweak current between meson states

Matrix element of weak current $J_\mu^W = \bar{c}\gamma_\mu(1-\gamma_5)b$ for $B_s \to D_s$ weak transitions:

$$\langle D_s(p_{D_s})|J_\mu^W|B_s(p_{B_s})\rangle = \int \frac{d^3p\, d^3q}{(2\pi)^6}\bar{\Psi}_{D_s\,\mathbf{p}_{D_s}}(\mathbf{p})\Gamma_\mu(\mathbf{p},\mathbf{q})\Psi_{B_s\,\mathbf{p}_{B_s}}(\mathbf{q})$$

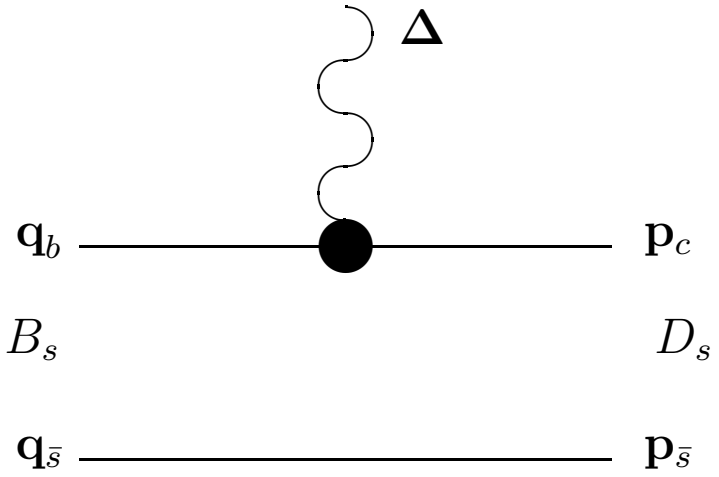

Figure 3: Lowest order vertex function $\Gamma^{(1)}(\mathbf{p},\mathbf{q})$ contributing to the current matrix element.

$$\Gamma_\mu^{(1)}(\mathbf{p},\mathbf{q}) = \bar{u}_c(p_c)\gamma_\mu(1-\gamma^5)u_b(q_b)(2\pi)^3\delta(\mathbf{p}_{\bar{s}}-\mathbf{q}_{\bar{s}})$$

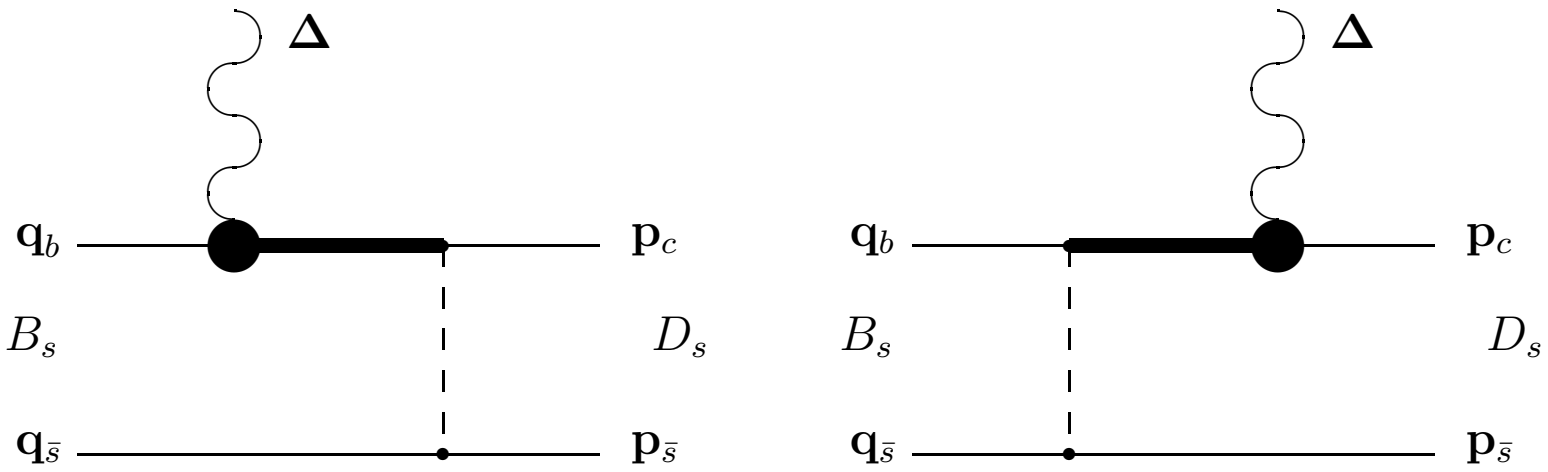

Figure 4: Vertex function $\Gamma^{(2)}(\mathbf{p},\mathbf{q})$ taking the quark interaction into account. Dashed lines correspond to the effective potential $\mathcal{V}$. Bold lines denote the negative-energy part of the quark propagator.

$$\Gamma^{(2)}_{\mu}(\mathbf{p},\mathbf{q}) = \bar{u}_c(p_c)\bar{u}_s(p_{\bar{s}})\Big\{\mathcal{V}(\mathbf{p}_{\bar{s}}-\mathbf{q}_{\bar{s}})\frac{\Lambda^{(-)}_c(k')}{\epsilon_c(k')+\epsilon_c(q_b)}\gamma^0_1\gamma_{1\mu}(1-\gamma^5_1)$$

$$+\gamma_{1\mu}(1-\gamma^5_1)\frac{\Lambda^{(-)}_b(k)}{\epsilon_b(k)+\epsilon_b(p_c)}\gamma^0_1\mathcal{V}(\mathbf{p}_{\bar{s}}-\mathbf{q}_{\bar{s}})\Big\}u_b(q_b)u_s(q_{\bar{s}})$$

$$\Lambda^{(-)}(p) = \frac{\epsilon(p)-\big(m\gamma^0+\gamma^0(\boldsymbol{\gamma}\mathbf{p})\big)}{2\epsilon(p)}, \qquad \epsilon(p)=\sqrt{\mathbf{p}^2+m^2}$$

$\mathbf{k}=\mathbf{p}_c-\boldsymbol{\Delta}; \qquad \mathbf{k}'=\mathbf{q}_b+\boldsymbol{\Delta}; \qquad \boldsymbol{\Delta}=\mathbf{p}_{D_s}-\mathbf{p}_{B_s}$

The wave function of a final D_s meson at rest is given by

$$\Psi_{D_s}(\mathbf{p}) \equiv \Psi^{JLS\mathcal{M}}_{D_{sJ}}(\mathbf{p}) = \mathcal{Y}^{JLS\mathcal{M}}\,\psi_{D_{sJ}}(\mathbf{p})$$

J and $\mathcal{M}$ — total meson angular momentum and its projection
L — orbital momentum
$S = 0, 1$ — total spin
$\psi_{D_{sJ}}(\mathbf{p})$ — radial part of the wave function

$$\mathcal{Y}^{JLS\mathcal{M}} = \sum_{\sigma_1\sigma_2} \langle L\,\mathcal{M} - \sigma_1 - \sigma_2,\ S\,\sigma_1 + \sigma_2 | J\,\mathcal{M}\rangle \langle \frac{1}{2}\,\sigma_1,\ \frac{1}{2}\,\sigma_2 | S\,\sigma_1 + \sigma_2\rangle Y_L^{\mathcal{M}-\sigma_1-\sigma_2}\chi_1(\sigma_1)\chi_2(\sigma_2)$$

The wave function of the moving meson $\Psi_{D_s\,\mathbf{\Delta}}$ is connected with the wave function in the rest frame $\Psi_{D_s\,\mathbf{0}} \equiv \Psi_{D_s}$ by the transformation

$$\Psi_{D_s\,\mathbf{\Delta}}(\mathbf{p}) = D_c^{1/2}(R^W_{L_{\mathbf{\Delta}}}) D_s^{1/2}(R^W_{L_{\mathbf{\Delta}}}) \Psi_{D_s\,\mathbf{0}}(\mathbf{p})$$

R^W — Wigner rotation
$L_{\mathbf{\Delta}}$ — Lorentz boost from the meson rest frame to a moving one
$D^{1/2}(R)$ — rotation matrix in spinor representation

$$\begin{pmatrix} 1 & 0 \\ 0 & 1 \end{pmatrix} D^{1/2}_{s,c}(R^W_{L_{\mathbf{\Delta}}}) = S^{-1}(\mathbf{p}_{\bar{s},c}) S(\mathbf{\Delta}) S(\mathbf{p})$$

$$S(\mathbf{p}) = \sqrt{\frac{\epsilon(p) + m}{2m}} \left(1 + \frac{\boldsymbol{\alpha}\mathbf{p}}{\epsilon(p) + m}\right)$$

$S(\mathbf{p})$ — usual Lorentz transformation matrix of Dirac spinor.

WEAK B_s DECAYS

• heavy-to-heavy decays	$B_s \to D_s l \nu_l$	$b \to c$ transition	CKM favored V_{cb}	$Br \sim 10^{-2}$
• heavy-to-light decays	$B_s \to K l \nu_l$	$b \to u$ transition	CKM suppressed V_{ub}	$Br \sim 10^{-4}$
• rare decays	$B_s \to \varphi(\eta) ll$	$b \to s$ transition	penguin diagrams $V_{tb}V_{ts}$	$Br \sim 10^{-6}$

Broad kinematical range:
the square of momentum transfer to the lepton pair q^2 varies
from 0 to $q^2_{\max} \approx 10$ GeV^2 for decays to D_s
from 0 to $q^2_{\max} \approx 20$ GeV^2 for decays to K and φ mesons
$\Longrightarrow$ the explicit determination of the q^2 dependence of the decay form factors in the whole kinematical range is needed

Large recoil of the final meson requires consistent relativistic treatment (e.g. boost of the meson wave functions from the rest to the moving reference frame)

Presence of heavy quarks in B_s and D_s mesons allows one to use expansions in the inverse powers of heavy quark masses $1/m_{b,c} \Longrightarrow$ significant simplifications, heavy quark symmetry relations can be used

Light u, d, s quarks should be treated relativistically

Large recoils allow one to neglect small relative momentum ($|\mathbf{p}|$) with respect to recoil ($|\mathbf{\Delta}|$) in the energies of light quarks in energetic light mesons $\epsilon_q(p+\Delta) \equiv \sqrt{m_q^2 + (\mathbf{p}+\mathbf{\Delta})^2} \longrightarrow \epsilon_q(\Delta) \equiv \sqrt{m_q^2 + \mathbf{\Delta}^2}$.
Such replacement is made in subleading contribution $\Gamma^{(2)}_\mu(\mathbf{p}, \mathbf{q})$ and permits the performance of one of the integrations using the quasipotential equation. As a result, the weak decay matrix element is expressed through the usual overlap integral of initial and final meson wave functions

Heavy-to-heavy semileptonic $B_s \to D_s$ decays

- **Decays to ground state D_s mesons**

HQET parametrization for the weak decay matrix elements:

$$\begin{aligned}
\frac{\langle D_s(v')|\bar{c}\gamma^\mu b|B_s(v)\rangle}{\sqrt{M_{D_s}M_{B_s}}} &= h_+(v+v')^\mu + h_-(v-v')^\mu \\
\langle D_s(v')|\bar{c}\gamma^\mu b\gamma_5|B_s(v)\rangle &= 0 \\
\frac{\langle D_s^*(v',\epsilon)|\bar{c}\gamma^\mu b|B_s(v)\rangle}{\sqrt{M_{D_s^*}M_{B_s}}} &= ih_V\varepsilon^{\mu\alpha\beta\gamma}\epsilon^*_\alpha v'_\beta v_\gamma \\
\frac{\langle D_s^*(v',\epsilon)|\bar{c}\gamma^\mu\gamma_5 b|B_s(v)\rangle}{\sqrt{M_{D_s^*}M_{B_s}}} &= h_{A_1}(w+1)\epsilon^{*\mu} - (h_{A_2}v^\mu + h_{A_3}v'^\mu)(\epsilon^*\cdot v)
\end{aligned}$$

$$w = v\cdot v' = \frac{M_{B_s}^2 + M_{D_s^{(*)}}^2 - q^2}{2M_{B_s}M_{D_s^{(*)}}}, \qquad q = p_{B_s} - p_{D_s^{(*)}}$$

In $m_Q \to \infty$ limit, all form factors are expressed through the single universal Isgur-Wise function $\xi(w)$

$$\begin{aligned}
h_+(w) &= h_{A_1}(w) = h_{A_3}(w) = h_V(w) = \xi(w) \\
h_-(w) &= h_{A_2}(w) = 0
\end{aligned}$$

$$\xi(w) = \sqrt{\frac{2}{w+1}}\lim_{m_Q\to\infty}\int\frac{d^3p}{(2\pi)^3}\bar{\Psi}_{D_s}\left(\mathbf{p} + 2\epsilon_s(p)\sqrt{\frac{w-1}{w+1}}\,\mathbf{e_\Delta}\right)\Psi_{B_s}(\mathbf{p}), \qquad \mathbf{e_\Delta} = \frac{\mathbf{\Delta}}{\sqrt{\mathbf{\Delta}^2}}$$

At $1/m_Q$ order four sudleading functions ξ_3, $\chi_{1,2,3}$ and one mass parameter $\bar{\Lambda}$ arise

$$\begin{aligned}
\xi_3(w) &= (\bar{\Lambda} - m_q)\left(1 + \frac{2\,w-1}{3\,w+1}\right)\xi(w) \\
\chi_1(w) &= \bar{\Lambda}\frac{w-1}{w+1}\xi(w) \\
\chi_2(w) &= -\frac{1}{32}\frac{\bar{\Lambda}}{w+1}\xi(w) \\
\chi_3(w) &= \frac{1}{16}\bar{\Lambda}\frac{w-1}{w+1}\xi(w)
\end{aligned}$$

$$\bar{\Lambda} = M - m_Q = \langle \epsilon_s \rangle$$

$$\xi(1) = 1, \qquad \chi_1(1) = \chi_3(1) = 0$$

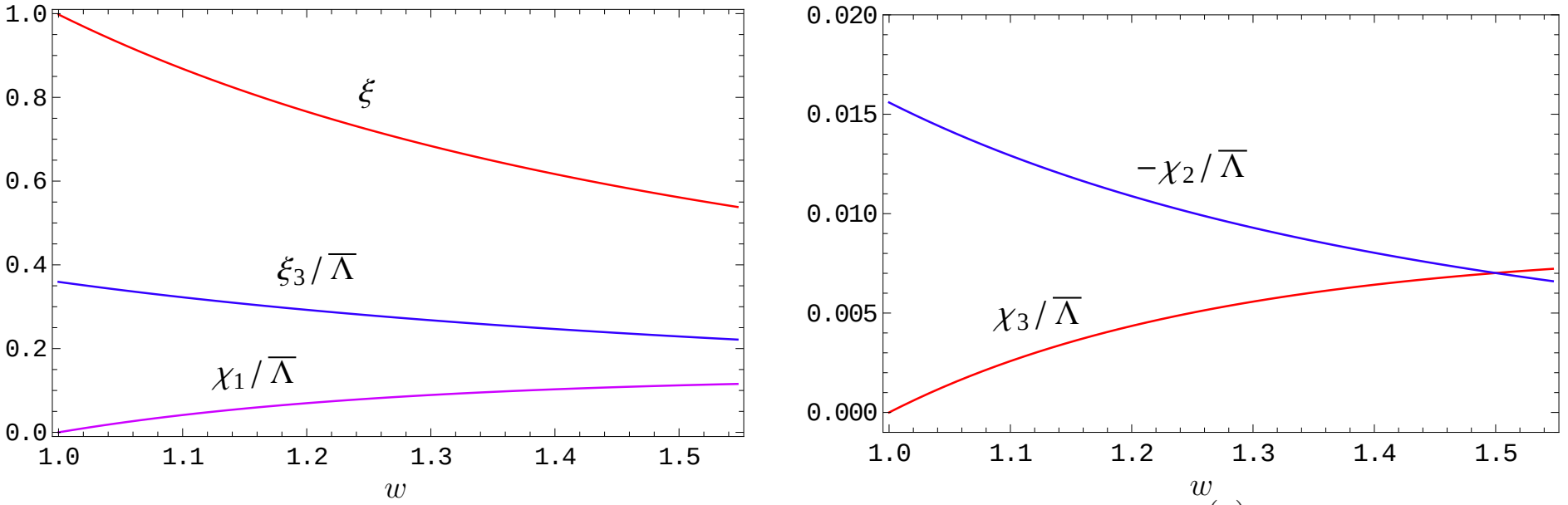

Figure 5: Leading and subleading Isgur-Wise functions for $B_s \to D_s^{(*)}$ transitions.

Other popular parametrization

$$\begin{aligned}
\langle D_s(p_{D_s})|\bar{c}\gamma^\mu b|B_s(p_{B_s})\rangle &= f_+(q^2)\left[p^\mu_{B_s}+p^\mu_{D_s}-\frac{M^2_{B_s}-M^2_{D_s}}{q^2}\,q^\mu\right]+f_0(q^2)\frac{M^2_{B_s}-M^2_{D_s}}{q^2}\,q^\mu \\
\langle D_s(p_{D_s})|\bar{c}\gamma^\mu\gamma_5 b|B_s(p_{B_s})\rangle &= 0 \\
\langle D^*_s(p_{D^*_s})|\bar{c}\gamma^\mu b|B(p_{B_s})\rangle &= \frac{2iV(q^2)}{M_{B_s}+M_{D^*_s}}\epsilon^{\mu\nu\rho\sigma}\epsilon^*_\nu p_{B_s\rho}p_{D^*_s\sigma} \\
\langle D^*_s(p_{D^*_s})|\bar{c}\gamma^\mu\gamma_5 b|B_s(p_{B_s})\rangle &= 2M_{D^*_s}A_0(q^2)\frac{\epsilon^*\cdot q}{q^2}\,q^\mu+(M_{B_s}+M_{D^*_s})A_1(q^2)\left(\epsilon^{*\mu}-\frac{\epsilon^*\cdot q}{q^2}\,q^\mu\right) \\
&\quad -A_2(q^2)\frac{\epsilon^*\cdot q}{M_{B_s}+M_{D^*_s}}\left[p^\mu_{B_s}+p^\mu_{D^*_s}-\frac{M^2_{B_s}-M^2_{D^*_s}}{q^2}\,q^\mu\right]
\end{aligned}$$

At the maximum recoil point ($q^2=0$)

$$f_+(0)=f_0(0)$$

$$A_0(0)=\frac{M_{B_s}+M_{D^*_s}}{2M_{D^*_s}}A_1(0)-\frac{M_{B_s}-M_{D^*_s}}{2M_{D^*_s}}A_2(0)$$

Table 1: Comparison of theoretical predictions for the form factors of semileptonic decays $B_s \to D_s^{(*)} e\nu$ at maximum recoil point $q^2 = 0$.

	$f_+(0)$	$V(0)$	$A_0(0)$	$A_1(0)$	$A_2(0)$
our	0.74 ± 0.02	0.95 ± 0.02	0.67 ± 0.01	0.70 ± 0.01	0.75 ± 0.02
Kramer (QM)	0.61	0.64		0.56	0.59
Blasi (SR)	0.7 ± 0.1	0.63 ± 0.05	0.52 ± 0.06	0.62 ± 0.01	0.75 ± 0.07
Chen (QM)	$0.57^{+0.02}_{-0.03}$	$0.70^{+0.05}_{-0.04}$		$0.65^{+0.01}_{-0.01}$	$0.67^{+0.01}_{-0.01}$
Li (LCSR)	$0.86^{+0.17}_{-0.15}$				
Li (QM)		$0.74^{+0.05}_{-0.05}$	$0.63^{+0.04}_{-0.04}$	$0.61^{+0.04}_{-0.04}$	$0.59^{+0.04}_{-0.04}$

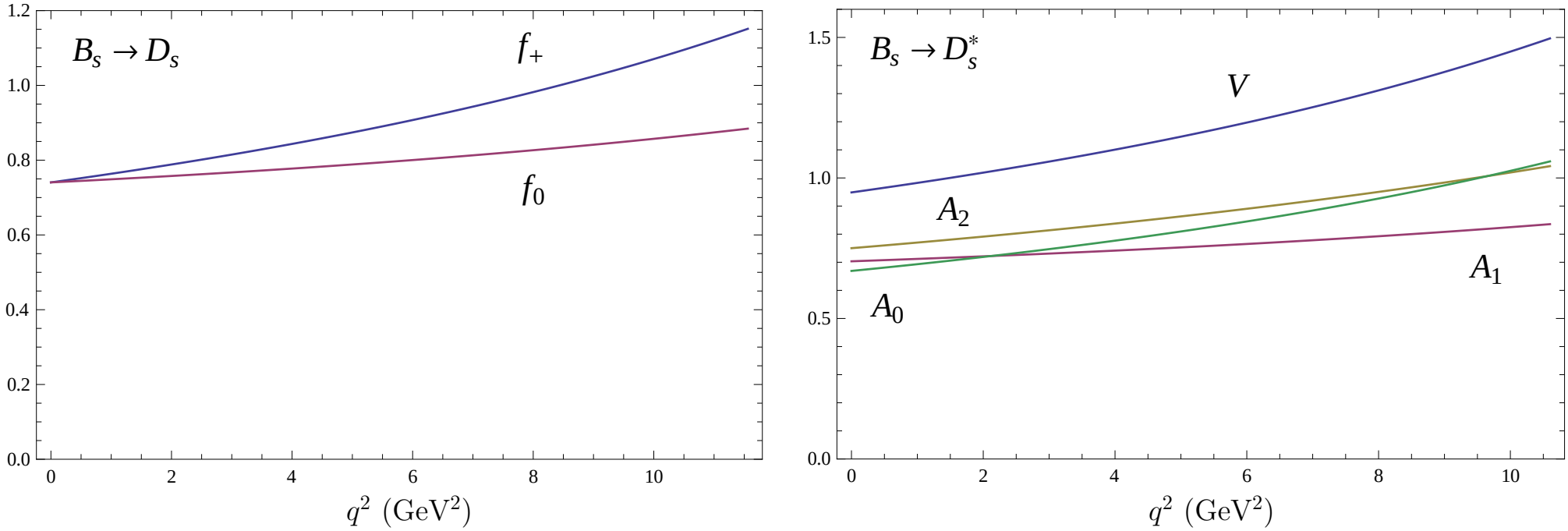

Figure 6: Form factors of weak $B_s \to D_s^{(*)}$ transitions.

Table 2: Comparison of theoretical predictions for the branching fractions of semileptonic decays $B_s \to D_s^{(*)} l\nu$ (in %).

Decay	our	SR Blasi	QM Chen	LCSR Li	QM Li	QM Zhao	SR Azizi
$B_s \to D_s e\nu$	2.1 ± 0.2	1.35 ± 0.21	1.4-1.7	$1.0^{+0.4}_{-0.3}$		2.73-3.00	2.8-3.8
$B_s \to D_s \tau\nu$	0.62 ± 0.05		0.47-0.55	$0.33^{+0.14}_{-0.11}$			
$B_s \to D_s^* e\nu$	5.3 ± 0.5	2.5 ± 0.1	5.1-5.8		5.2 ± 0.6	7.49-7.66	1.89-6.61
$B_s \to D_s^* \tau\nu$	1.3 ± 0.1		1.2-1.3		$1.3^{+0.2}_{-0.1}$		

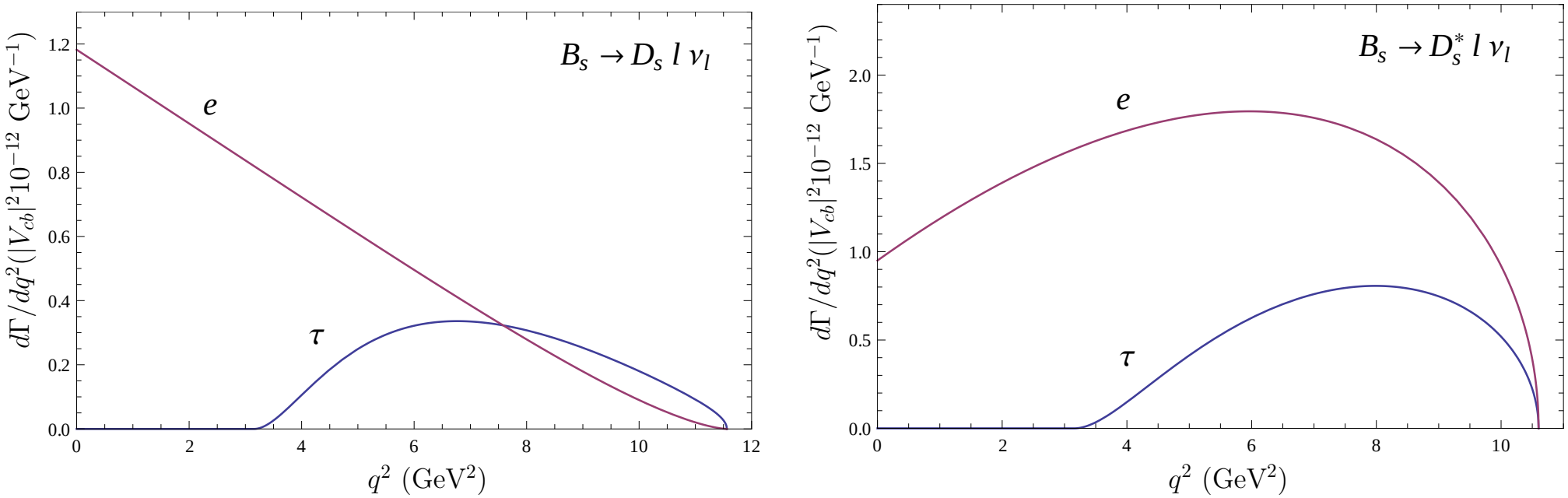

Figure 7: Predictions for the differential decay rates of the $B_s \to D_s^{(*)} l\nu$ semileptonic decays.

$$|V_{cb}| = (3.9 \pm 0.15) \times 10^{-2}$$

- **Decays to radially excited D_s mesons**

One leading $\xi^{(n)}$ and five subleading $\tilde{\xi}_3$, $\tilde{\chi}_{1,2,3,b}$ Isgur-Wise functions and two mass parameters $\bar{\Lambda} = M - m_Q$ and $\bar{\Lambda}^{(1)} = M(2S) - m_Q$ are required for the description of $B_s \to D_s^{(*)}(2S)$ decays

$$\xi^{(1)}(w) = \left(\frac{2}{w+1}\right)^{1/2} \int \frac{d^3p}{(2\pi)^3} \bar{\psi}^{(0)}_{D_s(2S)}\left(\mathbf{p} + 2\epsilon_s(p)\sqrt{\frac{w-1}{w+1}}\mathbf{e_\Delta}\right) \psi^{(0)}_{B_s}(\mathbf{p})$$

$$\tilde{\xi}_3(w) = \left(\frac{\bar{\Lambda}^{(1)} + \bar{\Lambda}}{2} - m_s + \frac{1}{6}\frac{\bar{\Lambda}^{(1)} - \bar{\Lambda}}{w-1}\right)\left(1 + \frac{2}{3}\frac{w-1}{w+1}\right)\xi^{(1)}(w)$$

$$\tilde{\chi}_1(w) \cong \frac{1}{20}\frac{w-1}{w+1}\frac{\bar{\Lambda}^{(1)} - \bar{\Lambda}}{w-1}\xi^{(1)}(w) + \frac{\bar{\Lambda}^{(1)}}{2}\left(\frac{2}{w+1}\right)^{1/2}\int \frac{d^3p}{(2\pi)^3}\bar{\psi}^{(1)si}_{D_s(2S)}\left(\mathbf{p} + 2\epsilon_s(p)\sqrt{\frac{w-1}{w+1}}\mathbf{e_\Delta}\right)\psi^{(0)}_{B_s}(\mathbf{p})$$

$$\tilde{\chi}_2(w) \cong -\frac{1}{12}\frac{1}{w+1}\frac{\bar{\Lambda}^{(1)} - \bar{\Lambda}}{w-1}\xi^{(1)}(w)$$

$$\tilde{\chi}_3(w) \cong -\frac{3}{80}\frac{w-1}{w+1}\frac{\bar{\Lambda}^{(1)} - \bar{\Lambda}}{w-1}\xi^{(1)}(w) + \frac{\bar{\Lambda}^{(1)}}{4}\left(\frac{2}{w+1}\right)^{1/2}\int \frac{d^3p}{(2\pi)^3}\bar{\psi}^{(1)sd}_{D_s(2S)}\left(\mathbf{p} + 2\epsilon_s(p)\sqrt{\frac{w-1}{w+1}}\mathbf{e_\Delta}\right)\psi^{(0)}_{B_s}(\mathbf{p})$$

$$\chi_b(w) \cong \bar{\Lambda}\left(\frac{2}{w+1}\right)^{1/2}\int \frac{d^3p}{(2\pi)^3}\bar{\psi}^{(0)}_{D_s(2S)}\left(\mathbf{p} + 2\epsilon_s(p)\sqrt{\frac{w-1}{w+1}}\mathbf{e_\Delta}\right)\left[\psi^{(1)si}_{B_s}(\mathbf{p}) - 3\psi^{(1)sd}_{B_s}(\mathbf{p})\right]$$

$$\psi_M = \psi^{(0)}_M + \frac{\bar{\Lambda}_M}{2m_Q}\left(\psi^{(1)si}_M + d_M\psi^{(1)sd}_M\right) + O(1/m_Q^2), \qquad d_P = -3, \quad d_V = 1$$

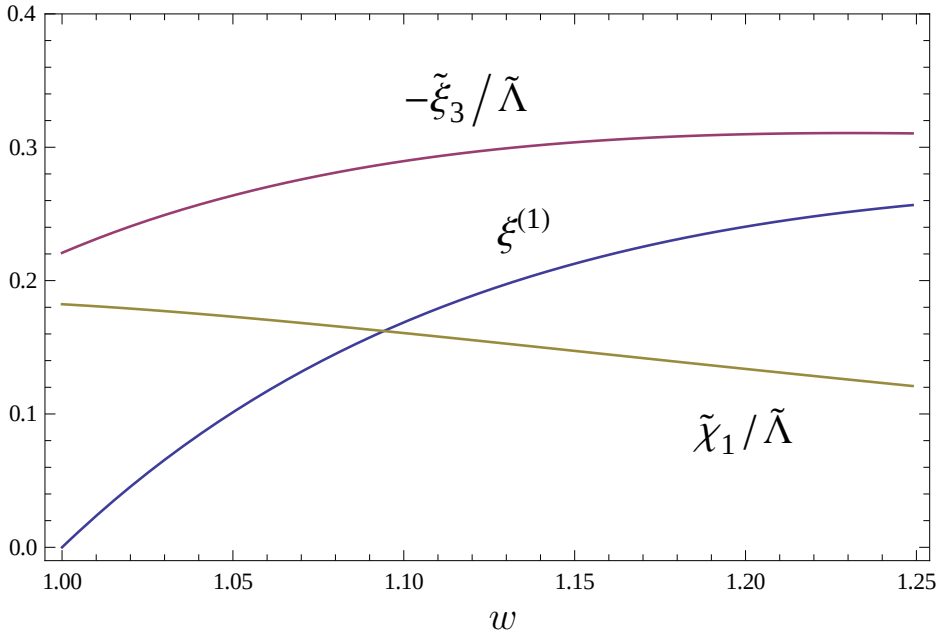

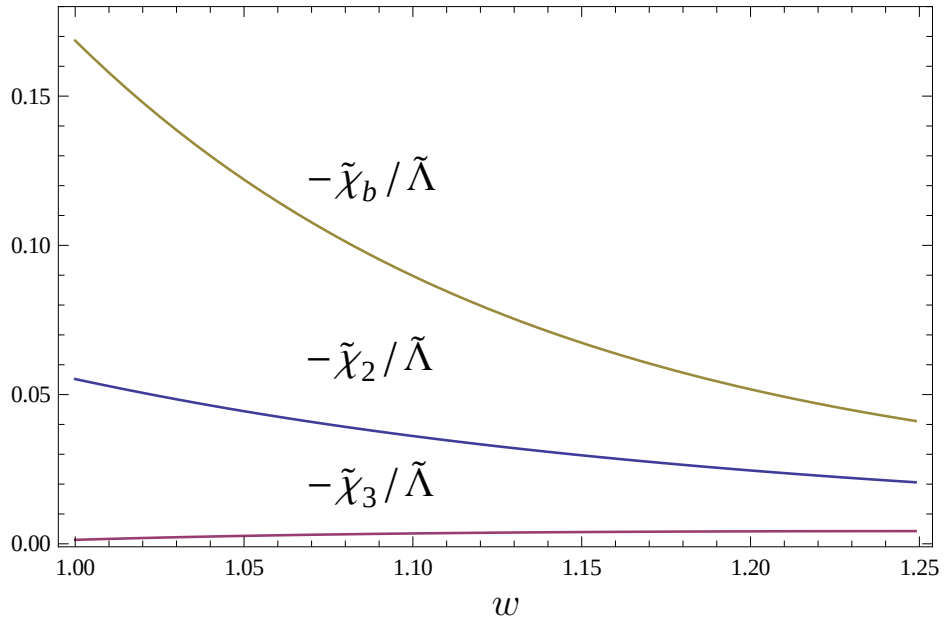

Figure 8: Leading and subleading Isgur-Wise functions for $B_s \to D_s^{(*)}(2S)$ transitions ($\tilde{\Lambda} = (\bar{\Lambda}^{(1)} + \bar{\Lambda})/2$).

Leading order Isgur-Wise function

$$\xi^{(1)}(1) = 0$$

since the radial parts of the wave functions $\Psi_{D_s(2S)}$ and Ψ_{B_s} are orthogonal in $m_Q \to \infty$ limit

Table 3: Predictions for the branching fractions of semileptonic decays $B_s \to D_s^{(*)}(2S)l\nu$ (in %).

Decay	Br
$B_s \to D_s(2S)e\nu$	0.27 ± 0.03
$B_s \to D_s(2S)\tau\nu$	0.011 ± 0.001
$B_s \to D_s^*(2S)e\nu$	0.38 ± 0.04
$B_s \to D_s^*(2S)\tau\nu$	0.015 ± 0.002

- **Decays to orbitally excited D_s mesons**

Parametrization of decay matrix elements through decay form factors

$$\langle D^*_{s0}(p_{D_{s0}})|\bar{c}\gamma^\mu b|B_s(p_{B_s})\rangle = 0$$

$$\langle D^*_{s0}(p_{D_{s0}})|\bar{c}\gamma^\mu\gamma_5 b|B(p_{B_s})\rangle = r_+(q^2)\left(p^\mu_{B_s}+p^\mu_{D_{s0}}\right)+r_-(q^2)\left(p^\mu_{B_s}-p^\mu_{D_{s0}}\right)$$

$$\langle D_{s1}(p_{D_{s1}})|\bar{c}\gamma^\mu b|B(p_{B_s})\rangle = (M_{B_s}+M_{D_{s1}})h_{V_1}(q^2)\epsilon^{*\mu}+[h_{V_2}(q^2)p^\mu_{B_s}+h_{V_3}(q^2)p^\mu_{D_{s1}}]\frac{\epsilon^*\cdot q}{M_{B_s}}$$

$$\langle D_{s1}(p_{D_{s1}})|\bar{c}\gamma^\mu\gamma_5 b|B(p_{B_s})\rangle = \frac{2ih_A(q^2)}{M_{B_s}+M_{D_{s1}}}\epsilon^{\mu\nu\rho\sigma}\epsilon^*_\nu p_{B_s\rho}p_{D_{s1}\sigma}$$

$$\langle D'_{s1}(p_{D_{s1}})|\bar{c}\gamma^\mu b|B(p_{B_s})\rangle = (M_{B_s}+M_{D'_{s1}})g_{V_1}(q^2)\epsilon^{*\mu}+[g_{V_2}(q^2)p^\mu_{B_s}+g_{V_3}(q^2)p^\mu_{D'_{s1}}]\frac{\epsilon^*\cdot q}{M_{B_s}}$$

$$\langle D_{s1}(p_{D_{s1}})|\bar{c}\gamma^\mu\gamma_5 b|B(p_{B_s})\rangle = \frac{2ig_A(q^2)}{M_{B_s}+M_{D'_{s1}}}\epsilon^{\mu\nu\rho\sigma}\epsilon^*_\nu p_{B_s\rho}p_{D'_{s1}\sigma}$$

$$\langle D^*_{s2}(p_{D_{s2}})|\bar{c}\gamma^\mu b|B(p_{B_s})\rangle = \frac{2it_V(q^2)}{M_{B_s}+M_{D_{s2}}}\epsilon^{\mu\nu\rho\sigma}\epsilon^*_{\nu\alpha}\frac{p^\alpha_{B_s}}{M_{B_s}}p_{B_s\rho}p_{D_{s2}\sigma}$$

$$\langle D^*_{s2}(p_{D_{s2}})|\bar{c}\gamma^\mu\gamma_5 b|B(p_{B_s})\rangle = (M_{B_s}+M_{D_{s2}})t_{A_1}(q^2)\epsilon^{*\mu\alpha}\frac{p_{B_s\alpha}}{M_{B_s}}+[t_{A_2}(q^2)p^\mu_{B_s}+t_{A_3}(q^2)p^\mu_{D_{s2}}]\epsilon^*_{\alpha\beta}\frac{p^\alpha_{B_s}p^\beta_{B_s}}{M^2_{B_s}}$$

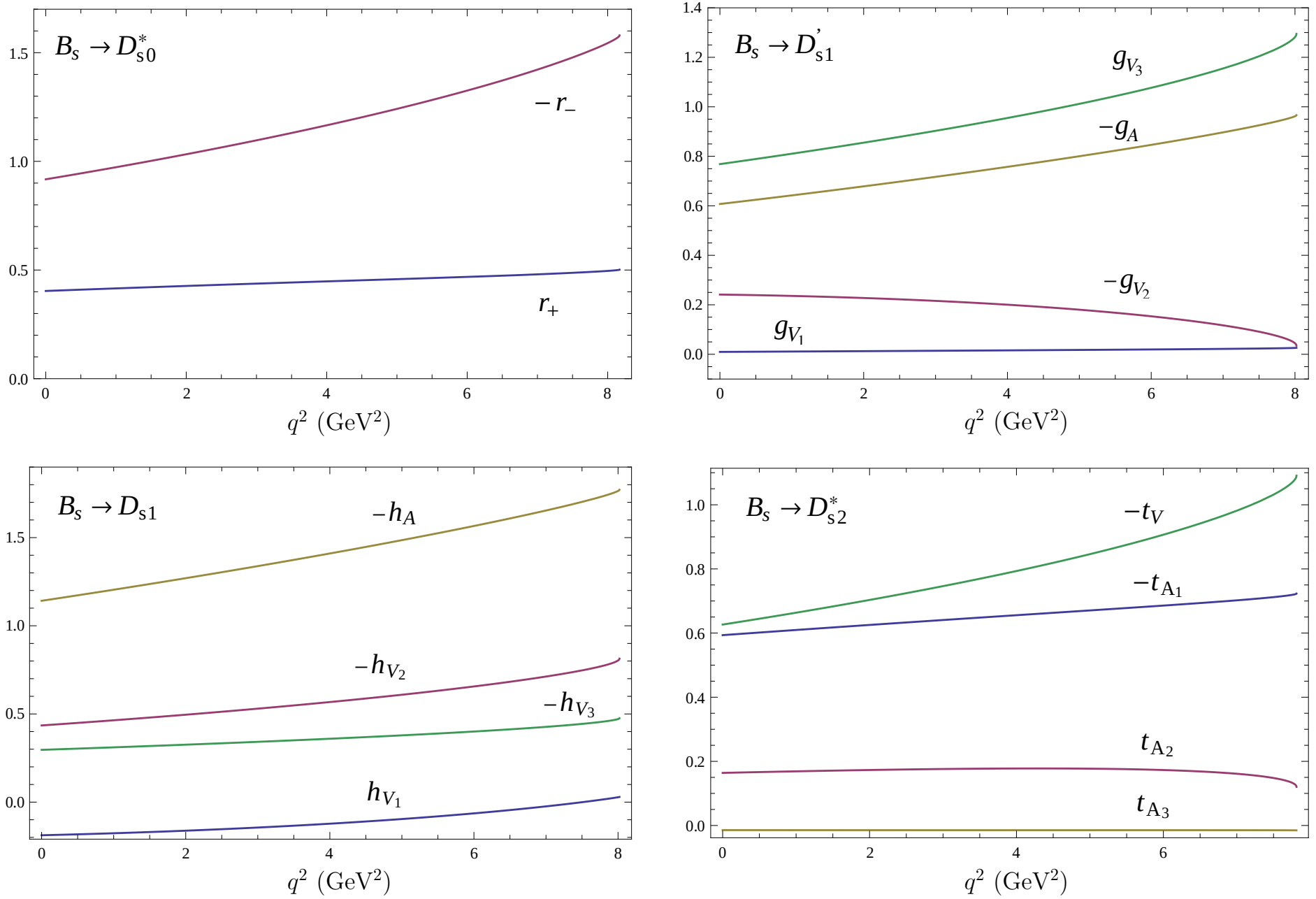

Figure 9: Form factors of the B_s decays to the P–wave $D^{(*)}_{sJ}$ mesons.

Table 4: Comparison of the predictions for the branching fractions of the semileptonic decays $B_s \to D_{sJ}^{(*)} l\nu$ (in %).

Decay	our	$m \to \infty$ with $1/m_Q$		QM	QM	LCSR	SR	HQET+SR
		EFG	EFG	Segovia	Zhao	Li	Aliev	Huang
$B_s \to D_{s0}^* e\nu$	0.36 ± 0.04	0.10	0.37	0.443	0.49-0.571	$0.23^{+0.12}_{-0.10}$	~ 0.1	0.20
$B_s \to D_{s0}^* \tau\nu$	0.019 ± 0.002					$0.057^{+0.028}_{-0.023}$	~ 0.01	
$B_s \to D'_{s1} e\nu$	0.19 ± 0.02	0.13	0.18	0.174-0.570	0.752-0.869		0.49	0.10
$B_s \to D'_{s1} \tau\nu$	0.015 ± 0.002							
$B_s \to D_{s1} e\nu$	0.84 ± 0.09	0.36	1.06	0.477				
$B_s \to D_{s1} \tau\nu$	0.049 ± 0.005							
$B_s \to D_{s2}^* e\nu$	0.67 ± 0.07	0.56	0.75	0.376				
$B_s \to D_{s2}^* \tau\nu$	0.029 ± 0.003							

Experimental data

$$Br(B_s \to D_{s1} X \mu\nu)_{\rm D0} = (1.03 \pm 0.20 \pm 0.17 \pm 0.14)\% \quad \text{(D0 Collaboration 2009)}$$

$$Br(B_s \to D_{s2}^* X \mu\nu)/Br(B_s \to X \mu\nu)_{\rm LHCb} = (3.3 \pm 1.0 \pm 0.4)\% \quad \text{(LHCb Collaboration 2011)}$$

$$Br(B_s \to D_{s1} X \mu\nu)/Br(B_s \to X \mu\nu)_{\rm LHCb} = (5.4 \pm 1.2 \pm 0.5)\%$$

$$Br(B_s \to D_{s2}^* X \mu\nu)/Br(B_s \to D_{s1} X \mu\nu)_{\rm LHCb} = 0.61 \pm 0.14 \pm 0.05$$

$$Br(B_s \to X \mu\nu)_{\rm theor} = Br(B_s \to D_s(1S, 2S)\mu\nu) + Br(B_s \to D_s(1P)\mu\nu) = (10.2 \pm 1.0)\%$$

$$Br(B_s \to D_{s2}^* \mu\nu)/Br(B_s \to X \mu\nu)_{\rm theor} = (6.5 \pm 1.2)\%$$
$$Br(B_s \to D_{s1} \mu\nu)/Br(B_s \to X \mu\nu)_{\rm theor} = (8.2 \pm 1.6)\%$$
$$Br(B_s \to D_{s2}^* \mu\nu)/Br(B_s \to D_{s1} \mu\nu)_{\rm theor} = 0.79 \pm 0.14$$

Total semileptonic $B_s \to D_s$ branching ratios

- for decays to ground state $D_s^{(*)}$ mesons

$$Br(B_s \to D_s^{(*)} e\nu) = (7.4 \pm 0.7)\%$$

$$Br(B_s \to D_s^{(*)} \tau\nu) = (1.92 \pm 0.15)\%$$

- for decays to orbitally excited $D_{sJ}^{(*)}$ mesons

$$Br(B_s \to D_{sJ}^{(*)} e\nu) = (2.1 \pm 0.2)\%$$

$$Br(B_s \to D_{sJ}^{(*)} \tau\nu) = (0.11 \pm 0.01)\%$$

- for decays to radially excited $D_s^{(*)}(2S)$ mesons

$$Br(B_s \to D_s^{(*)}(2S) e\nu) = (0.65 \pm 0.06)\%$$

$$Br(B_s \to D_s^{(*)}(2S) \tau\nu) = (0.026 \pm 0.003)\%$$

Branching fractions significantly decrease with excitation $\Longrightarrow$ Considered decays give the dominant contribution to the total semileptonic branching fraction

$$Br(B_s \to D_s e\nu + \text{anything}) = (10.2 \pm 1.0)\%$$

Experimental value (PDG)

$$Br(B_s \to D_s e\nu + \text{anything})_{\text{Exp.}} = (7.9 \pm 2.4)\%$$

Heavy-to-light semileptonic $B_s \to K$ decays

- **Decays to ground state K mesons**

Tensor weak current matrix elements

$$\begin{aligned}
\langle K(p_K)|\bar{q}\sigma^{\mu\nu}q_\nu b|B_s(p_{B_s})\rangle &= \frac{if_T(q^2)}{M_{B_s}+M_K}[q^2(p^\mu_{B_s}+p^\mu_K)-(M^2_{B_s}-M^2_K)q^\mu] \\
\langle K^*(p_{K^*})|\bar{q}i\sigma^{\mu\nu}q_\nu b|B_s(p_{B_s})\rangle &= 2T_1(q^2)\epsilon^{\mu\nu\rho\sigma}\epsilon^*_\nu p_{K^*\rho}p_{B_s\sigma} \\
\langle K^*(p_{K^*})|\bar{q}i\sigma^{\mu\nu}\gamma_5 q_\nu b|B_s(p_{B_s})\rangle &= T_2(q^2)[(M^2_{B_s}-M^2_{K^*})\epsilon^{*\mu}-(\epsilon^*\cdot q)(p^\mu_{B_s}+p^\mu_{K^*})] \\
&\quad +T_3(q^2)(\epsilon^*\cdot q)\left[q^\mu-\frac{q^2}{M^2_{B_s}-M^2_{K^*}}(p^\mu_{B_s}+p^\mu_{K^*})\right]
\end{aligned}$$

$$T_1(0)=T_2(0)$$

Table 5: Comparison of theoretical predictions for the form factors of weak $B_s \to K^{(*)}$ transitions at maximum recoil point $q^2=0$.

	$f_+(0)$	$f_T(0)$	$V(0)$	$A_0(0)$	$A_1(0)$	$A_2(0)$	$T_1(0)$	$T_3(0)$
our	0.284±0.014	0.236±0.012	0.291±0.015	0.289±0.015	0.287±0.015	0.286±0.015	0.238±0.012	0.122±0.006
LCSR	0.30±0.04		0.311±0.026	0.360±0.034	0.233±0.022	0.181±0.025	0.260±0.024	0.136±0.016
PQCD	0.24±0.05		0.21±0.04	0.25±0.05	0.16±0.04			
QM	0.31	0.31	0.38	0.37	0.29	0.26	0.32	0.23
PQCD			0.20±0.05	$0.24^{+0.07}_{-0.05}$	$0.15^{+0.04}_{-0.03}$	0.11±0.02	0.18±0.05	0.16±0.03
LCQM	0.290	0.317	0.323	0.279	0.232	0.210	0.271	0.165
LCSR	0.296±0.018	0.288±0.018	0.285±0.013	0.222±0.011	0.227±0.011	0.183± 0.010	0.251±0.012	0.169±0.008
QM	$0.260^{+0.055}_{-0.032}$		$0.227^{+0.064}_{-0.037}$	$0.280^{+0.090}_{-0.045}$	$0.178^{+0.047}_{-0.027}$			
PQCD	$0.26^{+0.05}_{-0.04}$	0.28±0.05						

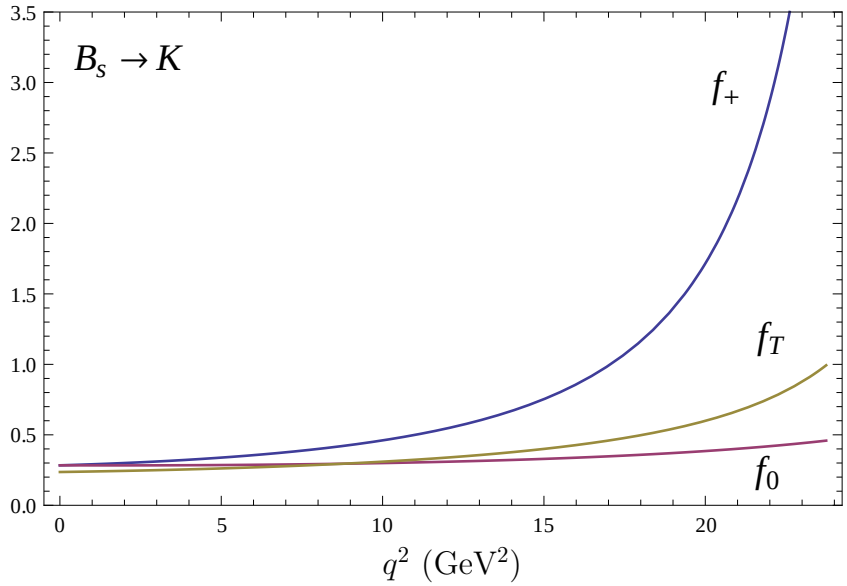

Figure 10: Form factors of the weak $B_s \longrightarrow K$ transition.

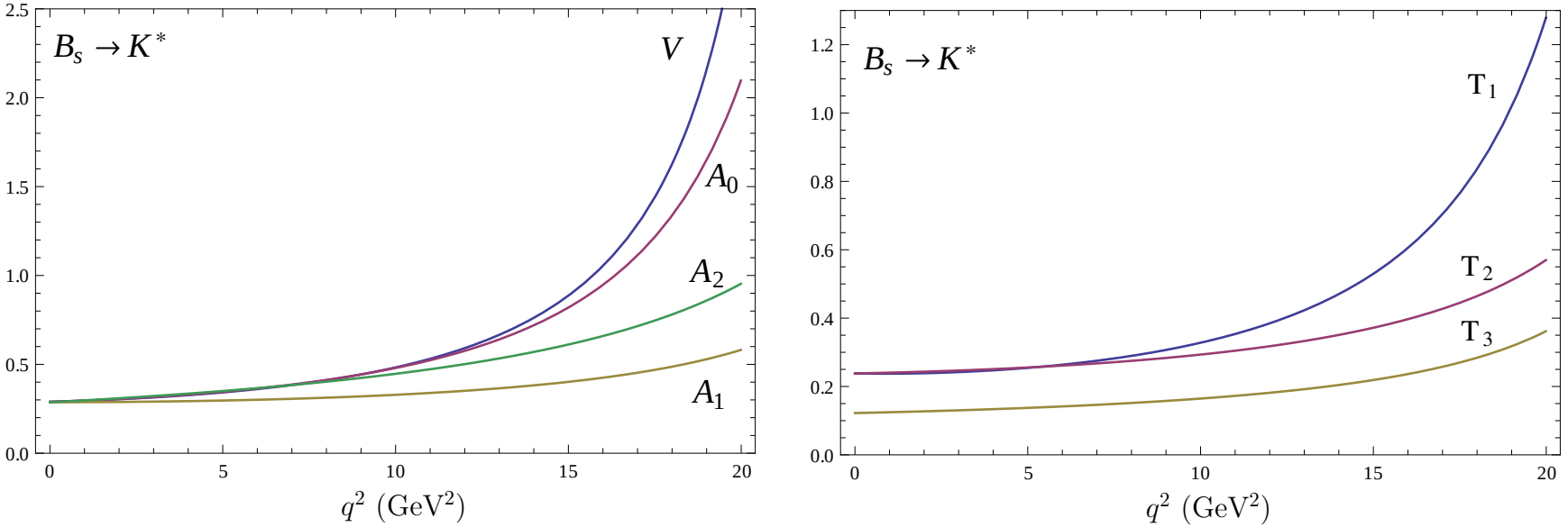

Figure 11: Form factors of the weak $B_s \longrightarrow K^*$ transition.

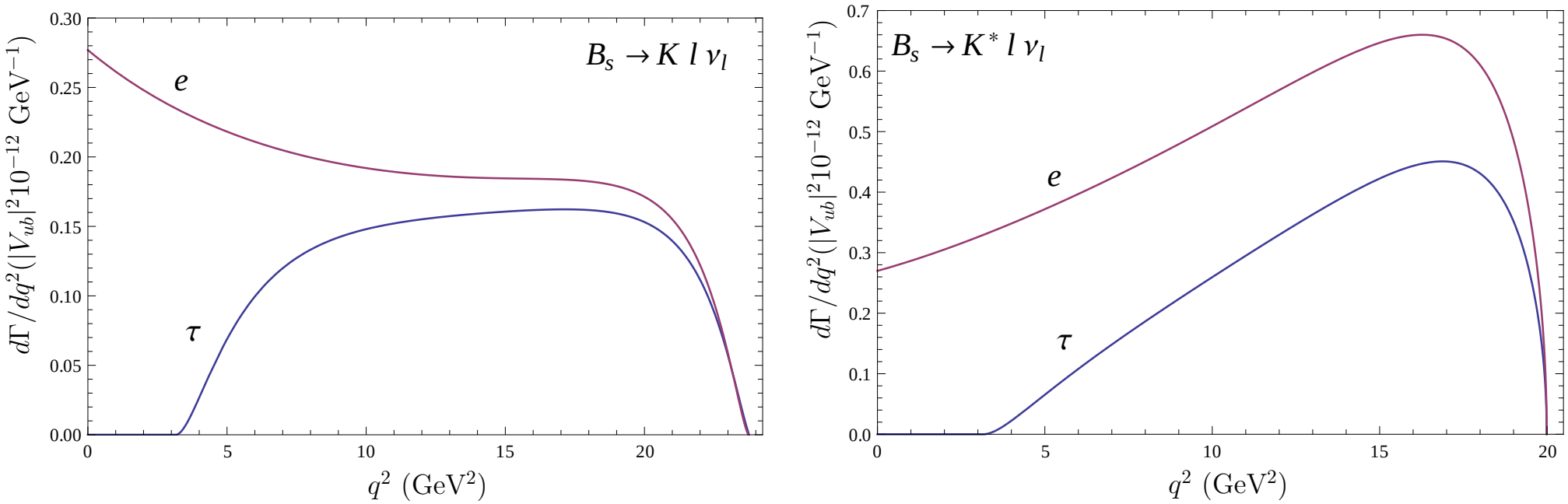

Figure 12: Predictions for the differential decay rates of the semileptonic $B_s \to K^{(*)} l\nu_l$ decays.

Table 6: Comparison of theoretical predictions for the branching fractions of semileptonic decays $B_s \to K^{(*)} l\nu_l$ (in 10^{-4}).

Decay	our	Wang (PQCD)	Wu (LCSR)
$B_s \to K e\nu_e$	1.64 ± 0.17	$1.27^{+0.49}_{-0.30}$	1.47 ± 0.15
$B_s \to K \tau\nu_\tau$	0.96 ± 0.10	$0.778^{+0.268}_{-0.201}$	1.02 ± 0.11
$B_s \to K^* e\nu_e$	3.47 ± 0.35		2.91 ± 0.26
$B_s \to K^* \tau\nu_\tau$	1.67 ± 0.17		1.58 ± 0.13

- **Decays to orbitally excited K mesons**

The P-wave K meson states with $J = L = 1$ are the mixtures of spin-triplet $(^3P_1)$ and spin-singlet $(^1P_1)$ states:

$$\begin{aligned} |K_1(1270)\rangle &= |K(^1P_1)\rangle \cos\varphi + |K(^3P_1)\rangle \sin\varphi \\ |K_1(1400)\rangle &= -|K(^1P_1)\rangle \sin\varphi + |K(^3P_1)\rangle \cos\varphi \end{aligned}$$

$\varphi = 43.8^\circ$ is a mixing angle determined from mass spectra calculations.

Table 7: Comparison of theoretical predictions for the form factors of the weak $B_s \to K_0^*$ transitions at the maximum recoil point $q^2 = 0$.

$F(0)$	our	Sun (LCSR)	Yang (SR)	Wang (LCSR)	Li (PQCD)	Han (SR)	Zhang (PQCD)
$r_+(0)$	0.27 ± 0.03	0.44	0.24 ± 0.10	$0.41^{+0.13}_{-0.07}$	$0.56^{+0.16}_{-0.13}$	0.39 ± 0.04	$0.56^{+0.07}_{-0.10}$
$r_-(0)$	-0.62 ± 0.06	-0.44		$-0.34^{+0.14}_{-0.09}$		-0.25 ± 0.05	

Table 8: Same as in Table 7 but for the $B_s \to K_1$ transitions.

$F(0)$	our	Yang (LCSR)	Li (PQCD)
$g_A(0)$	-0.33 ± 0.03	$-0.15^{+0.09}_{-0.07}$	0.03 ± 0.01
$g_{V_1}(0)$	-0.08 ± 0.01	$-0.11^{+0.07}_{-0.04}$	0.11 ± 0.07
$h_A(0)$	0.29 ± 0.03	0.49 ± 0.08	0.20 ± 0.05
$h_{V_1}(0)$	0.08 ± 0.01	0.38 ± 0.06	0.87 ± 0.25

Table 9: Same as in Table 7 but for the $B_s \to K_2^*$ transition.

$F(0)$	our	Wang (PQCD)
$t_V(0)$	-0.34 ± 0.03	$-0.18^{+0.05}_{-0.04}$
$t_{A_1}(0)$	-0.17 ± 0.02	$-0.11^{+0.03}_{-0.02}$

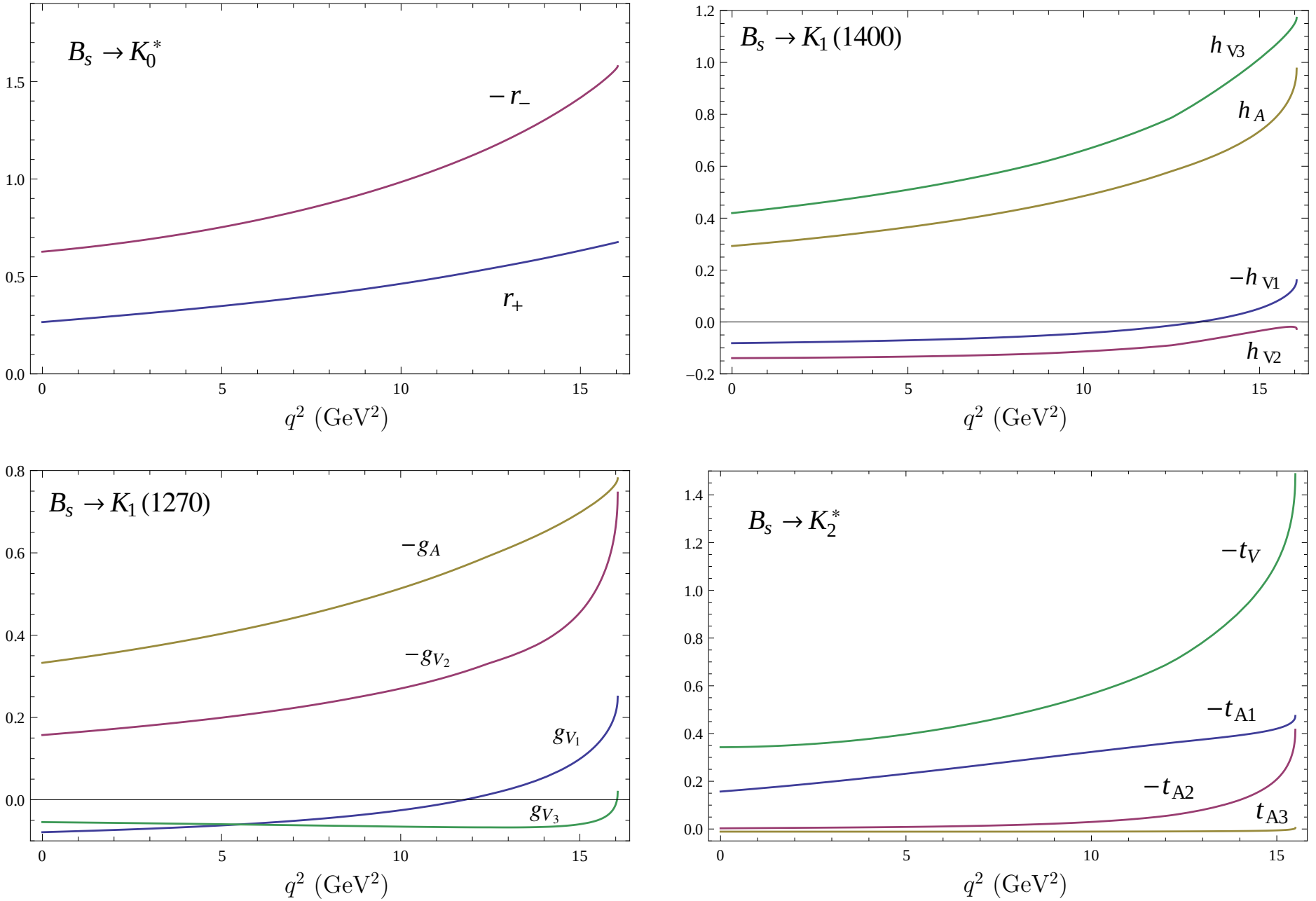

Figure 13: Form factors of the B_s decays to the P–wave $K_J^{(*)}$ mesons.

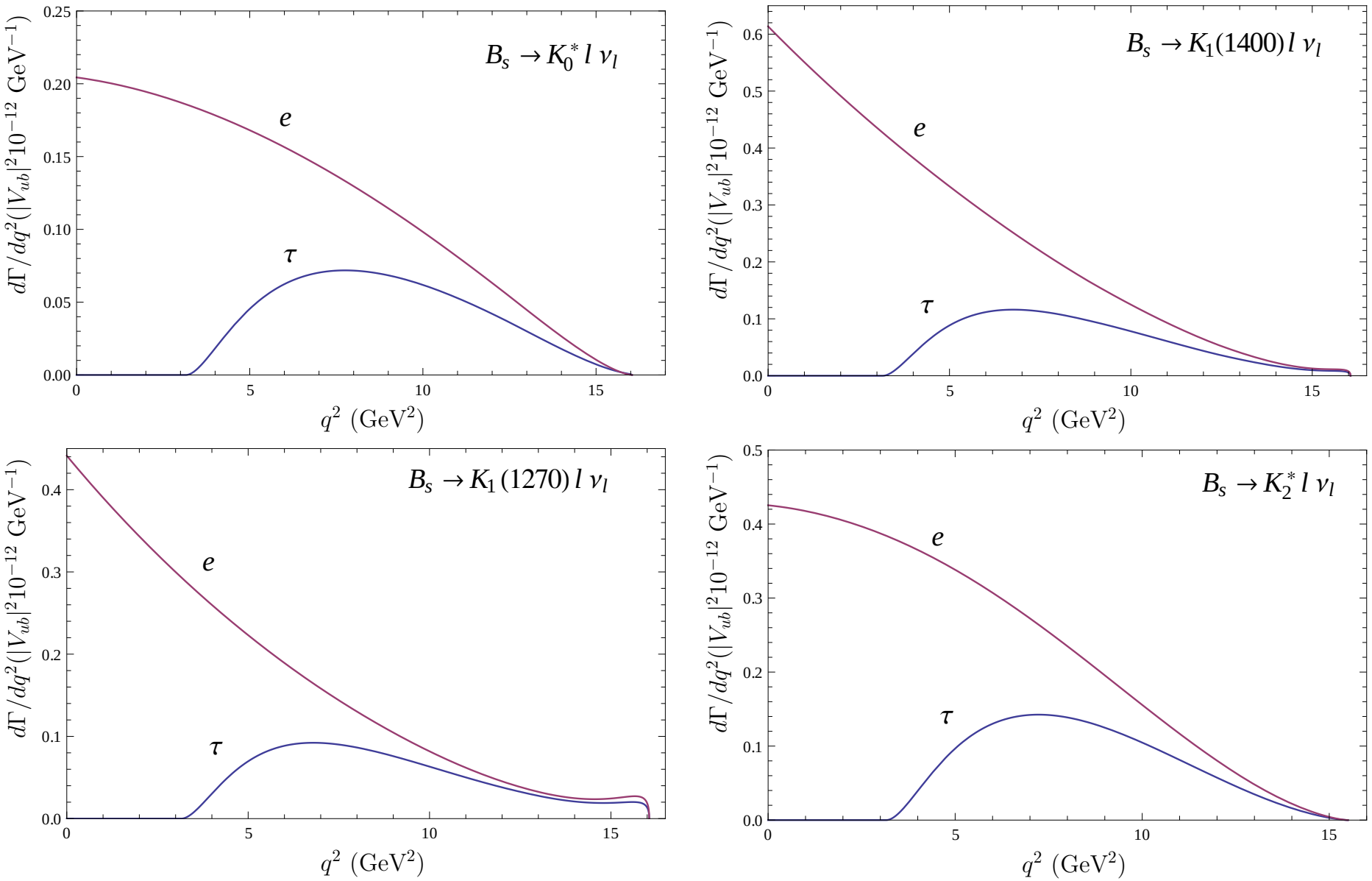

Figure 14: Predictions for the differential decay rates of the semileptonic $B \to K_J^{(*)} l \nu_l$ decays.

Table 10: Comparison of theoretical predictions for the branching fractions of semileptonic decays $B_s \to K_J^{(*)} l\nu_l$ (in 10^{-4}).

Decay	our	SR Yang	LCSR Wang	PQCD Li	LCSR Yang	PQCD Li	PQCD Wang
$B_s \to K_0^* e\nu_e$	0.71 ± 0.14	$0.36^{+0.38}_{-0.24}$	$1.3^{+1.3}_{-0.4}$	$2.45^{+1.77}_{-1.05}$			
$B_s \to K_0^* \tau\nu_\tau$	0.21 ± 0.04		$0.52^{+0.57}_{-0.18}$	$1.09^{+0.82}_{-0.47}$			
$B_s \to K_1(1270) e\nu_e$	1.41 ± 0.28				$4.53^{+1.67}_{-2.05}$	$5.75^{+3.49}_{-2.89}$	
$B_s \to K_1(1270) \tau\nu_\tau$	0.30 ± 0.06					$2.62^{+1.58}_{-1.31}$	
$B_s \to K_1(1400) e\nu_e$	0.97 ± 0.20				$3.86^{+1.43}_{-1.75}$	$0.03^{+0.05}_{-0.02}$	
$B_s \to K_1(1400) \tau\nu_\tau$	0.25 ± 0.05					$0.01^{+0.02}_{-0.01}$	
$B_s \to K_2^* e\nu_e$	1.33 ± 0.27						$0.73^{+0.48}_{-0.33}$
$B_s \to K_2^* \tau\nu_\tau$	0.36 ± 0.07						$0.25^{+0.17}_{-0.12}$

Total semileptonic B_s decays

- to ground state K mesons

$$Br(B_s \to K^{(*)} e\nu_e) = (5.11 \pm 0.51) \times 10^{-4}$$

$$Br(B_s \to K^{(*)} \tau\nu_\tau) = (2.63 \pm 0.26) \times 10^{-4}$$

- to first orbital excitations of K mesons

$$Br(B_s \to K_J^{(*)} e\nu_e) = (4.4 \pm 0.9) \times 10^{-4}$$

$$Br(B_s \to K_J^{(*)} \tau\nu_\tau) = (1.1 \pm 0.2) \times 10^{-4}$$

Branching fractions slightly decrease with excitation in contrast to the case of semileptonic $B_s \to D_s$ decays

$$Br(B_s \to K(1S, 1P) e\nu_e)_{\text{theor}} = (9.5 \pm 1.0) \times 10^{-4}$$

$Br(B_s \to X e\nu_e)_{\text{theor}} = (10.3 \pm 1.0)\%$ $\quad$ $Br(B_s \to X e\nu_e)_{\text{Exp.}} = (9.5 \pm 2.7)\%$ (PDG)

Rare B_s decays

- **Rare semileptonic $B_s \to \varphi(\eta)$ decays**

Table 11: Comparison of theoretical predictions for the form factors of weak $B_s \to \eta_s$ and $B_s \to \varphi$ transitions at maximum recoil point $q^2 = 0$.

	$f_+(0)$	$f_T(0)$	$V(0)$	$A_0(0)$	$A_1(0)$	$A_2(0)$	$T_1(0)$	$T_3(0)$
our	0.384 ± 0.019	0.301 ± 0.015	0.406 ± 0.020	0.322 ± 0.016	0.320 ± 0.016	0.318 ± 0.016	0.275 ± 0.014	0.133 ± 0.006
LCSR			0.434 ± 0.035	0.474 ± 0.033	0.311 ± 0.030	0.234 ± 0.028	0.349 ± 0.033	0.175 ± 0.018
PQCD	0.36 ± 0.07		0.25 ± 0.05	0.30 ± 0.06	0.19 ± 0.04			
RQM			0.32		0.29	0.28	0.28	
QM	0.36	0.36	0.44	0.42	0.34	0.31	0.38	0.26
PQCD			0.26 ± 0.07	$0.31^{+0.08}_{-0.07}$	$0.18^{+0.06}_{-0.05}$	0.12 ± 0.03	$0.23^{+0.06}_{-0.05}$	$0.19^{+0.06}_{-0.05}$
LCQM	0.288		0.329	0.279	0.232	0.210	0.276	0.170
LCSR	0.281 ± 0.015	0.282 ± 0.016	0.339 ± 0.017	0.269 ± 0.014	0.271 ± 0.014	0.212 ± 0.011	0.299 ± 0.016	0.191 ± 0.010
LFQM	0.357	0.365	0.445		0.343	0.310	0.380	
QM			$0.259^{+0.082}_{-0.037}$	$0.311^{+0.098}_{-0.049}$	$0.194^{+0.054}_{-0.029}$			

$$
\begin{aligned}
|\eta\rangle &= |\eta_q\rangle \cos\varphi - |\eta_s\rangle \sin\varphi \\
|\eta'\rangle &= |\eta_q\rangle \sin\varphi + |\eta_s\rangle \cos\varphi
\end{aligned}
$$

We use the experimental value

$$\varphi = (41.5 \pm 0.3 \pm 0.7 \pm 0.6)^\circ \qquad \text{(KLOE)}$$

and neglect the possible glue content

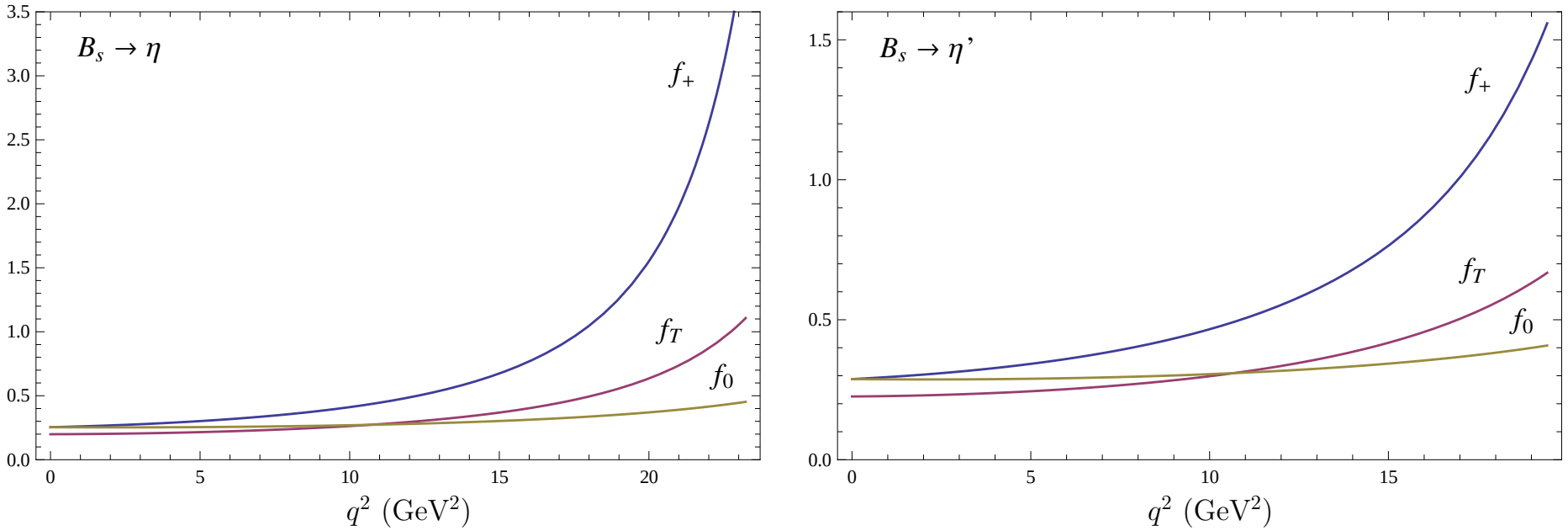

Figure 15: Form factors of the weak $B_s \longrightarrow \eta$ and $B_s \longrightarrow \eta'$ transitions.

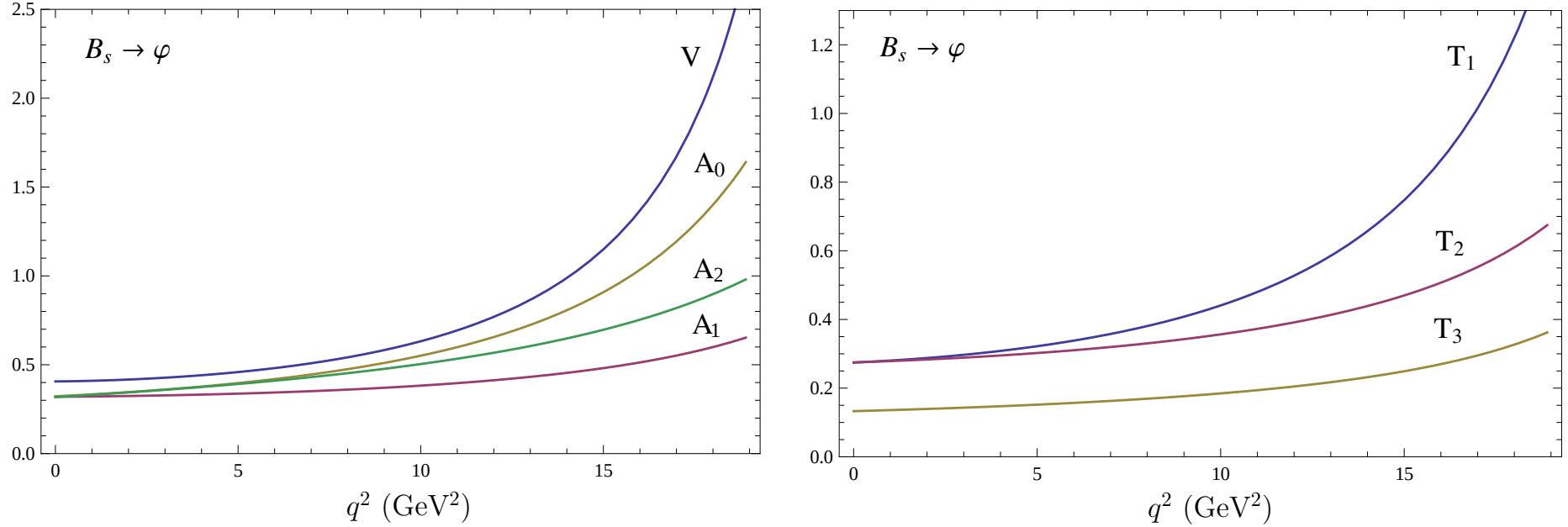

Figure 16: Form factors of the weak $B_s \longrightarrow \varphi$ transitions.

Free quark rare decay amplitude

$$
\begin{aligned}
M(b \to s l^+ l^-) &= \frac{G_F}{\sqrt{2}} \frac{\alpha}{2\pi} V_{ts}^* V_{tb} \Big[c_9^{\rm eff} (\bar{s}\gamma_\mu (1-\gamma_5) b)(\bar{l}\gamma^\mu l) + c_{10} (\bar{s}\gamma_\mu (1-\gamma_5) b)(\bar{l}\gamma^\mu \gamma_5 l) \\
&\quad - \frac{2 m_b}{q^2} c_7^{\rm eff} (\bar{s}\sigma_{\mu\nu} q^\nu (1+\gamma_5) b)(\bar{l}\gamma^\mu l) \Big] \\
M(b \to s \nu \bar{\nu}) &= \frac{G_F}{\sqrt{2}} \frac{\alpha}{2\pi} V_{ts}^* V_{tb} c_L^\nu (\bar{s}\gamma_\mu (1-\gamma_5) b)(\bar{\nu}\gamma^\mu (1-\gamma_5) \nu)
\end{aligned}
$$

The effective Wilson coefficient

$$
c_9^{\rm eff} = c_9 + \mathcal{Y}_{\rm pert}(q^2) + \mathcal{Y}_{\rm BW}(q^2)
$$

the perturbative part:

$$
\begin{aligned}
\mathcal{Y}_{\rm pert}(q^2) &= h\left(\frac{m_c}{m_b}, \frac{q^2}{m_b^2}\right)(3c_1 + c_2 + 3c_3 + c_4 + 3c_5 + c_6) \\
&\quad - \frac{1}{2} h\left(1, \frac{q^2}{m_b^2}\right)(4c_3 + 4c_4 + 3c_5 + c_6) \\
&\quad - \frac{1}{2} h\left(0, \frac{q^2}{m_b^2}\right)(c_3 + 3c_4) + \frac{2}{9}(3c_3 + c_4 + 3c_5 + c_6)
\end{aligned}
$$

the long-distance (nonperturbative) contributions originate from the $c\bar{c}$ resonances ($J/\psi, \psi' \ldots$) and have a phenomenological Breit-Wigner structure:

$$
\mathcal{Y}_{\rm BW}(q^2) = \frac{3\pi}{\alpha^2} \sum_{V_i = J/\psi, \psi'} \frac{\Gamma(V_i \to l^+ l^-) M_{V_i}}{M_{V_i}^2 - q^2 - i M_{V_i} \Gamma_{V_i}}.
$$

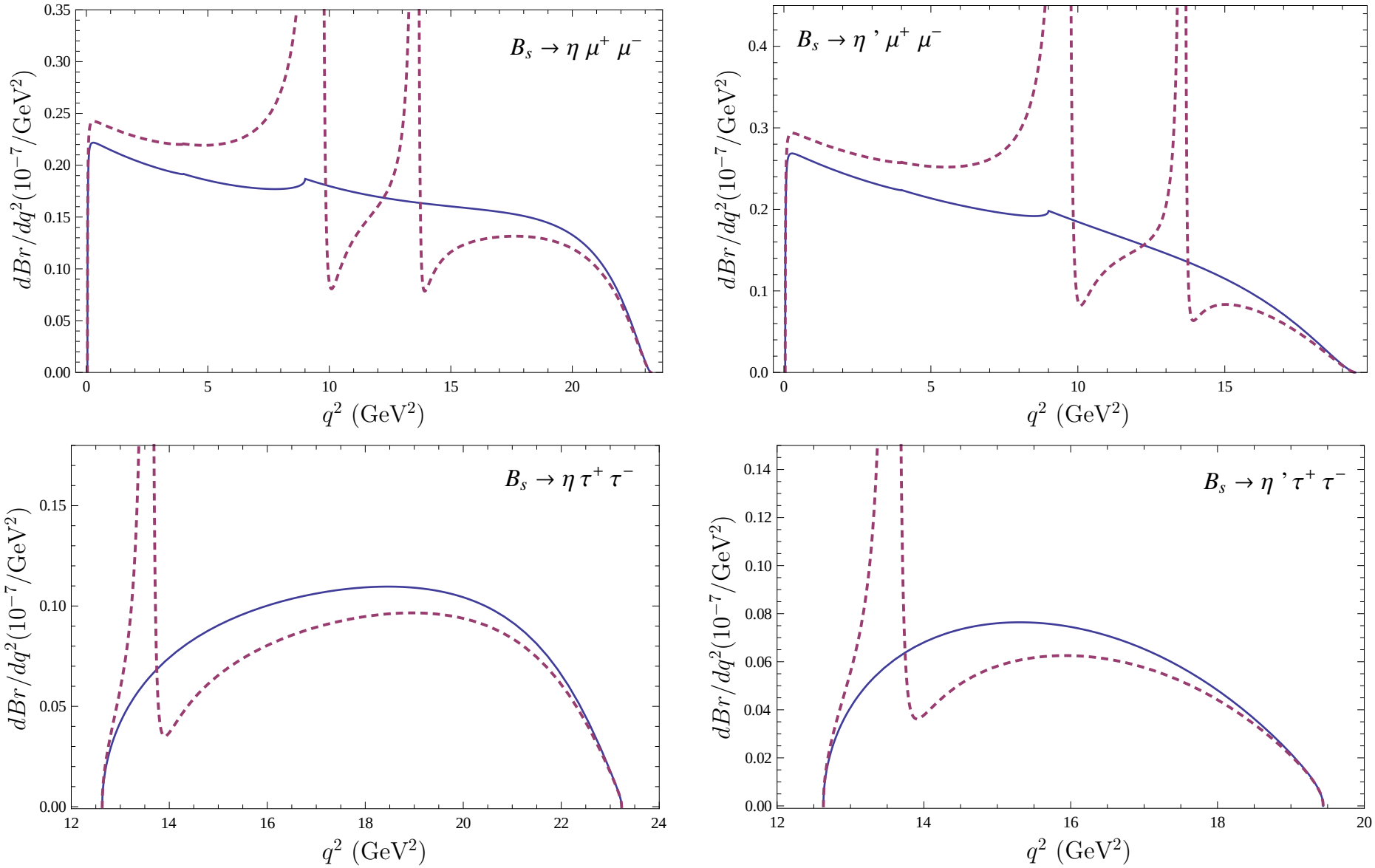

Figure 17: Theoretical predictions for the differential branching fractions $dBr(B_s \to \eta^{(\prime)} l^+ l^-)/dq^2$. Nonresonant and resonant results are plotted by solid and dashed lines, respectively.

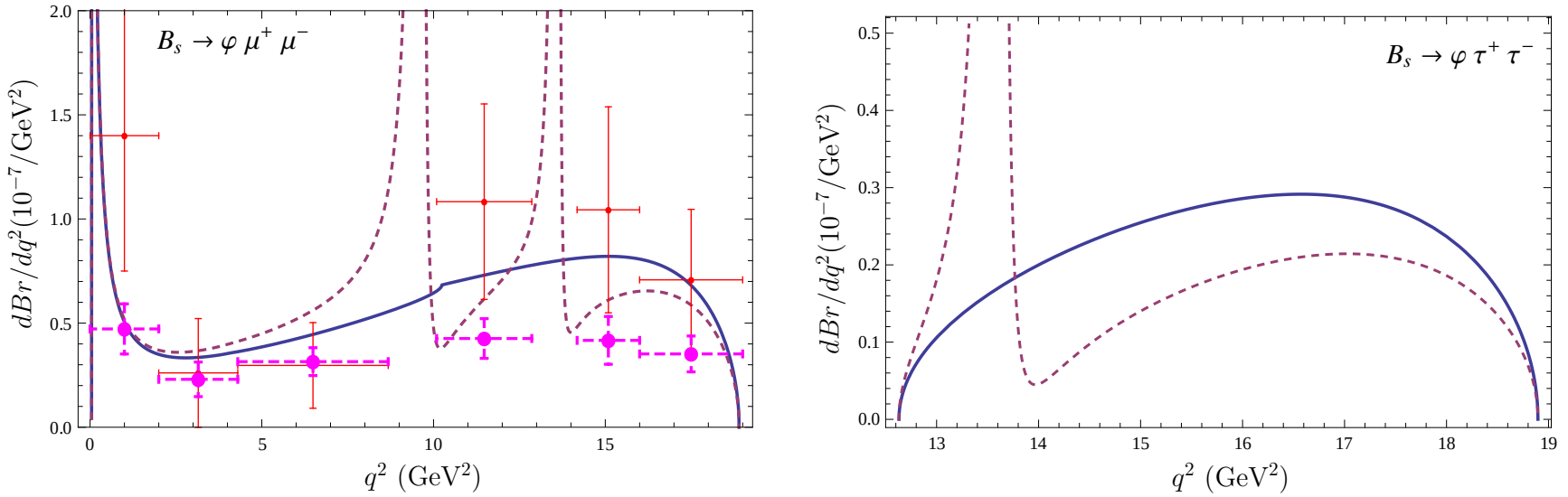

Figure 18: Comparison of theoretical predictions for the differential branching fractions $dBr(B_s \to \varphi\mu^+\mu^-)/dq^2$ with available experimental data. CDF data are given by dots with solid error bars, while LHCb data are presented by filled circles with dashed error bars.

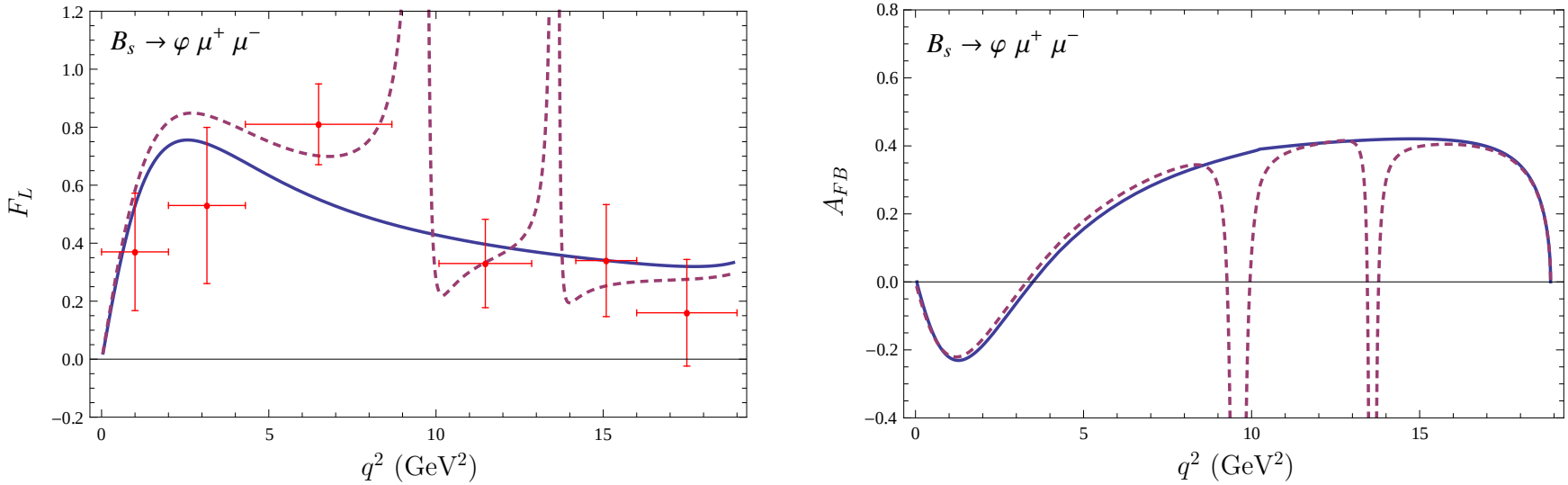

Figure 19: Comparison of theoretical predictions for the φ longitudinal polarization F_L and muon forward-backward asymmetry A_{FB} for the rare $B_s \to \varphi\mu^+\mu^-$ decays with available experimental data. LHCb data are given by dots with solid error bars.

Table 12: Comparison of theoretical predictions for the nonresonant branching fractions of the rare semileptonic B_s decays and available experimental data (in 10^{-7}).

Decay	our	LCSR	LFQM	SR	LFQM	LCSR	Experiment	
		Carlucci	Geng	Azizi	Choi	Wu	PDG	LHCb
$B_s \to \eta\mu^+\mu^-$	3.8 ± 0.4	3.4 ± 1.8	3.12	2.30 ± 0.97	2.4	1.2 ± 0.12		
$B_s \to \eta\tau^+\tau^-$	0.90 ± 0.09	1.0 ± 0.55	0.67	0.373±0.156	0.58	0.34 ± 0.04		
$B_s \to \eta\nu\bar{\nu}$	23.1 ± 2.3	29 ± 15	21.7	13.5 ± 5.6	17			
$B_s \to \eta'\mu^+\mu^-$	3.2 ± 0.3	2.8 ± 1.5	3.42	2.24 ± 0.94	1.8			
$B_s \to \eta'\tau^+\tau^-$	0.39 ± 0.04	0.47±0.25	0.43	0.280±0.118	0.26			
$B_s \to \eta'\nu\bar{\nu}$	19.7 ± 2.0	24 ± 13	23.8	13.3 ± 5.5	13			
$B_s \to \varphi\mu^+\mu^-$	11.6 ± 1.2		16.4			11.8 ± 1.1	$12.3^{+4.0}_{-3.4}$	$7.07^{+0.97}_{-0.94}$
$B_s \to \varphi\tau^+\tau^-$	1.5 ± 0.2		1.51			1.23 ± 0.11		
$B_s \to \varphi\nu\bar{\nu}$	79.6 ± 8.0		116.5				<54000	
$B_s \to K\mu^+\mu^-$	0.24 ± 0.03				0.14	0.199±0.021		
$B_s \to K\tau^+\tau^-$	0.059±0.006				0.03	0.074±0.007		
$B_s \to K\nu\bar{\nu}$	1.42 ± 0.14				1.01			
$B_s \to K^*\mu^+\mu^-$	0.44 ± 0.05					0.38 ± 0.03		
$B_s \to K^*\tau^+\tau^-$	0.075±0.008					0.050±0.004		
$B_s \to K^*\nu\bar{\nu}$	3.0 ± 0.3							

Table 13: Comparison of our predictions for the branching fractions of the rare semileptonic $B_s \to \varphi\mu^+\mu^-$ decays in several bins of q^2 with experimental data (in 10^{-7}).

q^2 bin (GeV^2)	our		PDG (CDF)	LHCb
	nonresonant	resonant		
$0.10 < q^2 < 2.00$	1.4 ± 0.2	1.4 ± 0.2	2.8 ± 1.3	0.944 ± 0.241
$2.00 < q^2 < 4.30$	0.79 ± 0.08	0.86 ± 0.09	0.6 ± 0.6	0.529 ± 0.191
$4.30 < q^2 < 8.68$	1.9 ± 0.2	2.6 ± 0.3	1.3 ± 0.9	1.38 ± 0.29
$10.09 < q^2 < 12.86$	2.0 ± 0.2	1.7 ± 0.2	3.0 ± 1.3	1.18 ± 0.26
$14.18 < q^2 < 16.00$	1.5 ± 0.2	1.1 ± 0.1	1.9 ± 0.9	0.759 ± 0.209
$16.00 < q^2$	1.8 ± 0.2	1.5 ± 0.2	2.3 ± 1.1	1.06 ± 0.26
$1.00 < q^2 < 6.00$	1.8 ± 0.2	2.0 ± 0.2	1.1 ± 0.9	1.14 ± 0.28
$0.10 < q^2 < 4.30$	2.2 ± 0.2	2.3 ± 0.2	3.3 ± 1.5	1.47 ± 0.23

- **Rare radiative B_s decays**

The exclusive rare radiative decay rate

$$\Gamma(B_s \to \varphi\gamma) = \frac{\alpha}{32\pi^4} G_F^2 m_b^2 M_{Bs}^3 |V_{tb}V_{ts}|^2 |c_7^{\rm eff}(m_b)|^2 |T_1(0)|^2 \left(1 - \frac{M_\varphi^2}{M_{Bs}^2}\right)^3 \left(1 + \frac{M_\varphi^2}{M_{Bs}^2}\right)$$

Table 14: Comparison of predictions for the branching fractions of the rare radiative decays with experimental data.

Decay	our	SCET	Experiment	
		Ali	PDG	LHCb
$Br(B^0 \to K^{*0}\gamma) \times 10^5$	4.3 ± 0.4	4.3 ± 1.4	4.33 ± 0.15	
$Br(B_s \to \varphi\gamma) \times 10^5$	3.8 ± 0.4	4.3 ± 1.4	$5.7^{+2.2}_{-1.9}$	3.5 ± 0.4
$\frac{Br(B^0 \to K^{*0}\gamma)}{Br(B_s \to \varphi\gamma)}$	1.14 ± 0.12	1.0 ± 0.2	0.7 ± 0.3	1.23 ± 0.12
$Br(B_s \to K^{*0}\gamma) \times 10^5$	0.13 ± 0.02			

CONCLUSIONS

- Relativistic quark model provides efficient tool for calculating weak transition matrix elements (form factors) between meson states
  - Form factors are expressed through the overlap integrals of meson wave functions
  - Wave functions are obtained as solutions of the relativistic wave equation which correctly describes meson spectroscopy
  - Relativistic transformations of the wave functions and contributions of intermediate negative-energy states are consistently taken into account
  - The momentum dependence of form factors is explicitly determined in the whole accessible kinematical range without additional assumptions and extrapolations
- Form factors of heavy-to-heavy, heavy-to-light and rare B_s decays were calculated
- On this basis semileptonic decay rates of B_s mesons to the ground-state and excited D_s and K mesons were obtained
- Rare semileptonic B_s decays to η and φ mesons were considered
- Calculated decay rates agree well with available data with the values of the CKM matrix elements V_{cb} and V_{ub} previously found in our model from weak B decays
- Obtained decay form factors can be applied for the calculation of the nonleptonic B_s decay rates in the factorization approximation